Hindered Transport of Large Molecules in Liquid-Filled Pores

Transport in liquid-filled pores of molecular dimensions plays an important role in membrane separations, in various forms of chromatography, and in catalysis, to name a few examples. A frequent observation is that if the pore dimensions are of the same order as those of a solute molecule, the apparent diffusion coefficient of that solute is much lower than in bulk solution. Likewise, rates of convective transport of such solutes are generally lower than the product of bulk concentration and volume flow rate. Thus, solute transport is typically "hindered" or restricted. A key objective of research on hindered transport is to be able to predict the applicable transport coefficients from such fundamental information as the size, shape, and electrical charge of the solutes and pores. The present status of this research is reviewed.

W. M. Deen
Department of Chemical Engineering
Massachusetts Institute of Technology
Cambridge, MA 02139

Introduction

In many situations of technological or scientific interest the dimensions of the solute molecule are at least several times greater than those of the solvent. In such cases the resistance to Brownian motion of the solute may be equated to the hydrodynamic drag on a particle of equivalent size and shape. For spherical solutes this leads to the Stokes-Einstein equation (Einstein, 1956):

$$D_\infty = \frac{kT}{6\pi\eta r_s} \tag{1}$$

where D_∞ is the diffusivity in dilute bulk solution, k is Boltzmann's constant, T is temperature, η is the solvent viscosity, and r_s is the radius of the solute. For nonspherical solutes of known D_∞, the value of r_s inferred from Eq. 1 is termed the Stokes-Einstein radius, the radius of a sphere of equal diffusivity. Solutes frequently behave as hydrodynamic particles with no slip at their surfaces, even when their radii are as small as two to three times that of the solvent. This is evidenced by the fact that under these circumstances, the Wilke-Chang correlation for binary diffusivities (Reid et al., 1987) is equivalent to Eq. 1. The hydrodynamic basis for Eq. 1, and its limitations, are well summarized in a review by Russel (1981).

For solutes that are large enough to behave as hydrodynamic particles, the phenomenon of hindered diffusion can be explained in part by the fact that the constrained space of a pore causes the molecular friction coefficient to exceed its value for an unbounded solution (denominator of Eq. 1). Analogous hydrodynamic constraints arise in convective transport through pores. In addition, because driving forces are usually expressed in terms of concentrations in the adjacent bulk solutions, the magnitudes of the corresponding transport coefficients are affected by factors that influence the equilibrium partitioning of solutes between pores and bulk solution, including steric exclusion. Steric restrictions and long-range intermolecular forces also affect the radial distribution of solutes within a pore, which in turn influences the hydrodynamic interactions between the solutes and pore wall.

Efforts to elucidate the selectivity of porous membranes using hydrodynamic models of hindered transport date back more than half a century. One of the earliest influential studies was that of Ferry (1936), who derived hindrance factors for convective transport from steric considerations. Hydrodynamic terms to describe reductions in solute mobility within pores were introduced by Pappenheimer et al. (1951) and Renkin (1954). The principal objective of these and many subsequent studies was to understand the permeability properties of biological structures such as the walls of blood capillaries. Many applications of theories of hindered transport to biological membranes during the 1950's and 1960's were reviewed by Solomon (1968). Some more recent physiological applications (with emphasis on the kidney microcirculation) have been reviewed by Deen et al. (1979). The concept of steric and/or hydrodynamic hindrances to transport in fine pores has found extensive use also in separations and reaction engineering. The diversity of such applications may be illustrated by a few examples: the characterization

of hemodialysis membranes (Klein et al., 1979), the modeling of size-exclusion (Casassa and Tagami, 1969) and hydrodynamic (Prieve and Hoysan, 1978) chromatography, the determination of an optimal pore size for supported catalysts (Ruckenstein and Tsai, 1981), and the assessment of diffusional limitations in the immobilization of enzymes on porous supports (Hossain et al., 1986).

The early 1970's saw a renewed interest in the theory of molecular motion through fine pores, stimulated in large part by the development of track-etch processes for making membranes with pores that are straight, of uniform cross section, and of near-molecular dimensions (Fleischer et al., 1972; Bean et al., 1970; Quinn et al., 1972). (Track-etch processes are described in the Appendix, note 1.) This provided for the first time an opportunity to directly test the theoretical predictions in model membranes having precisely known properties. Bean (1972) and Anderson and Quinn (1974) reviewed existing models of hindered transport and extended the theory in important ways, primarily in the treatment of the hydrodynamic hindrance factors. They and their associates also provided some critical experimental tests of one of the fundamental assumptions of hydrodynamic models of hindered transport, that the usual continuum equations for conservation of momentum (using the viscosity of bulk solvent) remain applicable in very small pores. Bean (1972), using track-etched mica membranes, showed that similar pore diameters could be inferred from diffusion of isotopically labeled water, bulk flow of water, and visualization by electron microscopy, even in the smallest pores tested (radius about 150Å). Anderson and Quinn (1972) compared pore sizes in track-etched mica membranes calculated from Knudsen flow of gases and from conductivity measurements, assuming in the latter bulk ionic mobilities. Excellent agreement was seen down to the minimum pore radius that could be examined, about 30Å. Together with other data on the temperature dependence of transport properties (Bean, 1972; Anderson and Quinn, 1972), these results strongly suggest that the viscosity of water in pores of those sizes does not deviate significantly from its bulk value. A direct test of diffusional hindrances in track-etched membranes was provided at about the same time by Beck and Schultz (1972). These theoretical and experimental contributions did much to lay the groundwork for subsequent studies.

During the past decade there has been a great deal of progress in further defining the hydrodynamics of molecular motion in pores, in quantifying the effects of electrostatic interactions, in understanding the effects of solute concentration on partitioning and transport coefficients, and in exploring the influence of molecular configuration on transport rates. The objective of the present review is to summarize this recent progress. The review is divided into three parts. Theoretical developments for rigid solutes are considered first, beginning with a discussion of diffusive and convective transport of dilute solutions of neutral spheres in cylindrical pores. Various extensions of the basic theory are then presented, which include electrostatic interactions, other pore shapes, nonspherical solutes, and finite solute concentrations. The second major part reviews experimental results obtained with rigid solutes in model membranes, including the effects of solute size and electrical charge on hindered diffusion, and studies of convective transport and osmosis. The third part deals with theories and data for flexible polymers—molecules that undergo random changes in shape and that are also subject to flow-induced deformation.

Theory for Hindered Transport of Rigid Solutes

Solute flux equations for spheres in cylindrical pores

A derivation of hindrance factors for diffusion and convection of rigid, spherical molecules in cylindrical pores will illustrate many of the theoretical issues involved. The steady state approach presented here parallels that of Anderson and Quinn (1974), but with more attention to the radial averaging process, in keeping with the more detailed analysis of Brenner and Gaydos (1977). The most basic assumption is that the radius of the pore r_0 and that of the solute molecules r_s greatly exceed that of the solvent, which is treated as a continuum. At the very low Reynolds numbers of interest, flow is fully developed within about one pore radius downstream from the entrance (Weinbaum, 1981). To employ fully developed velocity profiles, and also to neglect mass transfer resistances associated with pore entrances and exits (Malone and Anderson, 1978), the pore length L will be assumed to be much larger than its radius. The bulk solution is assumed first to be sufficiently dilute to neglect all solute-solute interactions. The behavior of nonspherical solutes and noncircular pores, and the effects of finite solute concentration, will be discussed subsequently. The initial physical situation can therefore be depicted as in Figure 1.

The velocity of a representative solute molecule will be taken to be a constant, U. Thus, it is assumed that random fluctuations in the motion of a given molecule have been averaged over a long time, or equivalently, over many identical molecules at a given instant. Such averaging also makes meaningful the concept of pointwise concentrations, which are simply proportional to the probabilities of finding particle centers at given locations. It should be emphasized that the schematic representation in Figure 1 illustrates only one instantaneous configuration. With $L/r_0 \gg 1$, a diffusing molecule will be able to "sample" all radial positions many times during passage through a pore. In the presence of bulk flow, such radial sampling will occur if the Peclet number based on pore radius is small.

In the average sense, the driving force for diffusion, the gradient in chemical potential, may be viewed as a body force on the solute molecule (Einstein, 1956). With the assumption of steady motion in an isothermal fluid, and neglecting other body forces (Lightfoot et al., 1976), this body force is exactly balanced by a hydrodynamic force, yielding

$$-kT\frac{\partial \ln C}{\partial z} - 6\pi\eta r_s K(U - GV) = 0 \qquad (2)$$

The first term in Eq. 2 represents the diffusional force per molecule in the $+z$ direction, and the second term is the correspond-

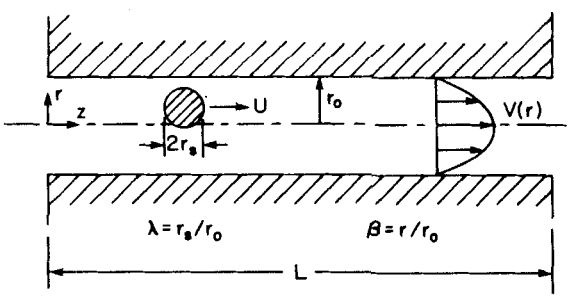

Figure 1. Spherical solute in a cylindrical pore.

ing hydrodynamic force. The solute concentration is denoted by C, and the unperturbed fluid velocity far upstream or downstream from the particle by V. The contribution of pressure variations to the gradient in chemical potential, usually negligible in the present context and ignored in Eq. 2, has been included by some authors (Lightfoot et al., 1976; Levitt, 1975a). The hydrodynamic coefficients K, the enhanced drag, and G, the lag coefficient, account for the effects of finite pore size. In an unbounded fluid, $K = G = 1$, and the second term is equivalent to Stokes' law. One effect of the pore walls is to increase the drag on a sphere translating parallel to the pore axis ($K > 1$). A second effect is to cause the velocity of a freely suspended sphere to lag behind the approach velocity of the fluid ($G < 1$), at any given radial position. The evaluation of K and G will be discussed later.

Noting that the solute flux is given by $N = UC$, Eq. 2 rearranges to

$$N = - K^{-1}D_\infty \frac{\partial C}{\partial z} + GVC \tag{3}$$

where D_∞ is given by Eq. 1. Thus, for the special case of a stagnant, unbounded fluid ($V = 0$, $K = 1$), this development provides an elementary derivation of the Stokes-Einstein equation (similar to that of Einstein, 1956, pp. 68–75). Equation 3 is the usual flux equation for a dilute liquid solution, but with the contributions from diffusion and convection modified by the factors K^{-1} and G, respectively. As will be discussed, both of these hydrodynamic coefficients depend on the ratio of solute radius to pore radius, $\lambda = r_s/r_0$, as well as on radial position within a pore. For a long cylindrical pore, the unperturbed fluid velocity has the parabolic profile:

$$V = 2\langle V\rangle(1 - \beta^2) \tag{4}$$

where $\langle V\rangle$ is the mean velocity and $\beta = r/r_0$ is dimensionless radial position.

Radial variations in C are of great importance. Their origin can be seen most readily by considering steric restrictions on the possible positions of a rigid sphere within a cylinder; since the solute center must always be at least a distance r_s from the pore wall, $C = 0$ for $\beta > 1 - \lambda$. Additional radial variations in C may be induced by long-range forces between the solute and pore wall.

Because of the dependence of C, V, K, and G on β, it is evident that N must also vary with radial position. A more useful quantity macroscopically is the flux averaged over the pore cross section, $\langle N\rangle$:

$$\langle N\rangle = \frac{\int_0^1 N\beta d\beta}{\int_0^1 \beta d\beta} = 2\int_0^{1-\lambda} N\beta d\beta \tag{5}$$

The new upper limit in the righthand integral of Eq. 5 comes from the fact that $N = 0$ in the annular region from which solute centers are excluded. It is desired to relate $\langle N\rangle$ first to the local cross-sectional average concentration $\langle C\rangle$ (definition analogous to $\langle N\rangle$), and ultimately to the more measurable concentrations in the bulk solutions bounding the pores.

Averaging Eq. 3 over the pore cross section yields

$$\langle N\rangle = - 2D_\infty \int_0^{1-\lambda} K^{-1}\frac{\partial C}{\partial z}\beta d\beta + 4\langle V\rangle \int_0^{1-\lambda} GC(1 - \beta^2)\beta d\beta \tag{6}$$

The righthand side of Eq. 6 can be converted to terms involving only $\langle C\rangle$ if it is assumed that the axial and radial dependences of C are separable. An appropriate form is

$$C = g(z)\exp[-E(\beta)/kT] \tag{7}$$

where E is a potential describing long range interactions (e.g., electrostatic forces) between the solute and the pore wall, which are assumed here to depend only on radial position. For $\langle V\rangle = 0$, Brenner and Gaydos (1977) have shown Eq. 7 to be consistent with the dynamics of a Brownian particle, provided that the particle has sufficient time to sample all radial positions within the pore. Equation 7 is not exact for $\langle V\rangle \neq 0$, and its use is equivalent to neglecting Taylor dispersion (Brenner and Gaydos, 1977). However, as will be discussed, Taylor dispersion is usually unimportant in hindered transport, so that Eq. 7 remains a good approximation.

Combining Eqs. 6 and 7, the desired local flux equation is obtained:

$$\langle N\rangle = - K_d D_\infty \frac{d\langle C\rangle}{dz} + K_c\langle V\rangle\langle C\rangle \tag{8}$$

$$K_d = \frac{\int_0^{1-\lambda} K^{-1}e^{-E/kT}\beta d\beta}{\int_0^{1-\lambda} e^{-E/kT}\beta d\beta} \tag{9}$$

$$K_c = \frac{2\int_0^{1-\lambda} G(1 - \beta^2)e^{-E/kT}\beta d\beta}{\int_0^{1-\lambda} e^{-E/kT}\beta d\beta} \tag{10}$$

The quantity $K_d D_\infty$ is an appropriately averaged intrapore diffusion coefficient, based on solute concentrations averaged over the pore cross section. K_d and K_c are equivalent to the quantities $\bar{d}_{11}$ and $\bar{u}^*$, respectively, defined by Brenner and Gaydos (1977).

Relating steady state fluxes to the concentrations in the adjacent external solutions (C_0 at $z = 0$ and C_L at $z = L$) requires that Eq. 8 be integrated over pore length. (For the accommodation of boundary-layer resistances, see Appendix, note 2.) With the assumption of long pores, the mass transfer resistances associated with the two-dimensional flows at the pore entrances and exits can be neglected. In this case, the concentrations just within the pores are essentially at equilibrium with the corresponding external concentrations. Choosing $E \equiv 0$ in the external solutions, elementary statistical thermodynamics implies that the probability of finding a solute molecule at a given radial position is proportional to $\exp[-E(\beta)/kT]$. This Boltzmann distribution of concentrations is consistent with Eq. 7, derived from dynamic considerations (Brenner and Gaydos, 1977), provided that one chooses $g(0) = C_0$ and $g(L) = C_L$. Doing this and

averaging over the pore cross section,

$$\Phi = \frac{\langle C\rangle_0}{C_0} = \frac{\langle C\rangle_L}{C_L} = 2\int_0^{1-\lambda} e^{-E/kT}\beta d\beta \tag{11}$$

where Φ is the partitioning or distribution coefficient, the ratio of the average intrapore concentration to that in bulk solution, at equilibrium. An important special case is that of purely steric interactions between the solute and pore wall ($E = 0$):

$$\Phi = (1 - \lambda)^2 \tag{12}$$

Equation 11 was given by Brenner and Gaydos (1977), and Eq. 12 has been obtained by various authors using either geometric (Renkin, 1954) or statistical thermodynamic arguments (Giddings et al., 1968).

The desired macroscopic flux equation is obtained finally by integrating Eq. 8, with boundary conditions from Eq. 11:

$$\langle N\rangle = W\langle V\rangle C_0 \frac{[1 - (C_L/C_0)e^{-Pe}]}{[1 - e^{-Pe}]} \tag{13}$$

$$Pe = \frac{W\langle V\rangle L}{HD_\infty} \tag{14}$$

$$H = \Phi K_d = 2\int_0^{1-\lambda} K^{-1}e^{-E/kT}\beta d\beta \tag{15}$$

$$W = \Phi K_c = 4\int_0^{1-\lambda} G(1 - \beta^2)e^{-E/kT}\beta d\beta \tag{16}$$

For $E = 0$, these results are identical to those given by Anderson and Quinn (1974), where H and W correspond to their ξ and χ, respectively. It can be seen that the effect of adopting bulk solution concentrations is to introduce the factor Φ in the hindrance coefficients.

The limiting forms of Eq. 13 for extremes of the Peclet number based on pore length, Pe, are

$$\langle N\rangle = \frac{HD_\infty}{L}(C_0 - C_L) \qquad (Pe \ll 1) \tag{17}$$

$$\langle N\rangle = W\langle V\rangle C_0 \qquad (Pe \gg 1) \tag{18}$$

Solute transport is dominated by diffusion for $Pe \ll 1$ and by convection for $Pe \gg 1$. These expressions establish a relationship between hindered transport theory and certain phenomenological transport coefficients for porous membranes. The "solute permeability" is proportional to HD_∞/L; with fluxes based as usual on total membrane area, the permeability would be given by $\gamma HD_\infty/L$, where γ is the fraction of the membrane surface occupied by pores. The "reflection coefficient" for filtration (convective transport of solute) is

$$\sigma_f = 1 - W \tag{19}$$

The reflection coefficient σ_f can be interpreted as the fraction of solute "reflected" or rejected by the membrane, when convection is dominant. Expressions for σ_f derived by Bean (1972), Levitt (1975a), and Lightfoot et al. (1976) are equivalent to Eqs. 16 and 19, with $E = 0$.

Osmosis

Although the main focus of this review is hindered transport of solutes, the closely related phenomenon of osmotic flow of fluid deserves some attention. A hydraulic permeability L_p and osmotic reflection coefficient σ_0 for a porous membrane can be defined by

$$J_v = \gamma\langle V\rangle = L_p(\Delta P - \sigma_0\Delta\Pi) \tag{20}$$

$$L_P = \frac{\gamma r_0^2}{8\eta L} \tag{21}$$

where ΔP and $\Delta\Pi$ are the differences in hydraulic and osmotic pressure, respectively, between the external solutions. For dilute solutions, $\Delta\Pi = RT(C_0 - C_L)$ from van't Hoff, where R is the gas constant. Equation 21 follows from Poiseuille flow for the special case $\Delta\Pi = 0$. The factor γ (pore area fraction) has been introduced by following the usual practice of basing the volume flux (J_v) on total membrane area.

For "ideal semipermeable" membranes, which permit passage of water but not solute, $\sigma_0 = 1$. The principal theoretical issue is the prediction of σ_0 for porous membranes that only partially reject solute. This problem has been approached by Anderson and coworkers (Anderson and Malone, 1974; Anderson, 1981; Adamski and Anderson, 1983; Anderson and Adamski, 1983) by focusing on pressure gradients induced by steric or other exclusion of macrosolutes from the region near the pore wall. Briefly stated, the gradient of the solute-pore wall potential was considered to provide a body force on the fluid in the radial direction, inducing radial variations in the isotropic stress (pressure) even in a static fluid. Since solute centers are excluded from the region $\beta > 1 - \lambda$, there is a discontinuity in this equivalent pressure at $\beta = 1 - \lambda$. Osmotic equilibrium of the solvent requires the pressure to be lower in the solute-free region near the wall. In the nonequilibrium situation, axial variations in solute concentration induce oppositely directed gradients in pressure within the solute-free region, resulting in bulk flow.

For the case of very dilute solutions, solute concentration profiles were assumed to be of the form of Eq. 7 (Anderson and Malone, 1974; Anderson, 1981). A consideration of stress variations in the pore due to solute-wall interactions leads to the following result (Anderson, 1981):

$$\sigma_0 = 1 - 4\int_0^{1-\lambda} e^{-E/kT}(1 - \beta^2)\beta d\beta \tag{22}$$

From Eqs. 16, 19, and 22, it can be seen that σ_0 differs from σ_f only in the absence of the factor $G(\lambda, \beta)$ in the integrand. For neutral solutes and pores ($E = 0$), Eq. 22 reduces to

$$\sigma_0 = (1 - \Phi)^2 \tag{23}$$

where Φ is given by Eq. 12. This remarkably simple result illustrates the close relationship between osmosis and the steric exclusion of solutes from membrane pores.

Eqs. 16, 19, and 22 imply a distinction between σ_f and σ_0, although quantitative differences are small (Anderson, 1981). Levitt (1975a) used a thermodynamic/hydrodynamic approach to evaluate σ_0, equating dissipation of free energy due to transport between reservoirs with dissipation of mechanical energy

within the pore. His results suggest that σ_0 is identical to σ_f, as given by Eqs. 16 and 19. The explanation for these subtle differences in σ_0 is not presently clear.

The interested reader is directed elsewhere for further discussion of the relationships between hindered transport theory and the phenomenological coefficients of nonequilibrium thermodynamics (Bean, 1972; Anderson and Quinn, 1974; Curry, 1974; Levitt, 1975a; Lightfoot et al., 1976; Anderson and Adamski, 1983).

Evaluation of hydrodynamic coefficients

Implementation of the theory of hindered transport has been handicapped to some extent by a lack of complete hydrodynamic information. As indicated by Eqs. 15 and 16, the hydrodynamic functions needed are $K(\lambda, \beta)$ and $G(\lambda, \beta)$. These can be determined, in principle, by computing the drag on a sphere translating parallel to the tube axis with $V = 0$, and by determining the velocity ratio U/V for a sphere freely suspended in a Poiseuille flow, both for vanishing Reynolds number. Results for a wide range of values of λ are available, however, only for the axisymmetric case (sphere on centerline, $\beta = 0$). Evidence that the centerline values, $K(\lambda, 0)$ and $G(\lambda, 0)$, may lead to reasonably accurate estimates for H and W (see below) has led to widespread use of the "centerline approximation." For $E = 0$, Eqs. 15 and 16 become

$$H \simeq \Phi K^{-1}(\lambda, 0) \tag{24}$$

$$W \simeq \Phi(2 - \Phi) G(\lambda, 0) \tag{25}$$

where Φ is given by Eq. 12. An early relation equivalent to Eq. 24 for the diffusional hindrance factor was given by Pappenheimer et al. (1951). Bean (1972) appears to have been the first to obtain Eq. 25. Ferry (1936) assumed in effect that $G = 1$, while Renkin (1954) assumed that $G = K^{-1}$. The earlier work of Pappenheimer et al. (1951) assumed that $W = H$.

As already noted, $K = G = 1$ for $\lambda \to 0$. As $\lambda \to 1$, $K^{-1}(\lambda, 0) \to 0$ and $G(\lambda, 0) \to \frac{1}{2}$; in this case the sphere moves as a piston, its center translating at velocity $U = \langle V \rangle = V(0)/2$. Values of $K^{-1}(\lambda, 0)$ and $G(\lambda, 0)$ have been evaluated numerically and presented in tabular form for $0 \le \lambda \le 0.9$ by Haberman and Sayre (1958), Wang and Skalak (1969), and Paine and Scherr (1975). Some of the analytical expressions that have been employed for H and W (all for $E = 0$) are summarized in Table 1. Entry (1) for H in the table was obtained using an approximation to $K^{-1}(\lambda, 0)$ that is accurate only for $\lambda < 0.4$ (Anderson and Quinn, 1974); it is equivalent to the commonly used "Renkin equation" (Renkin, 1954). Entry (1) for W has the same limitations on λ. Bean (1972) gave similar expressions, but included terms up to λ^{10} in the series representations of $K^{-1}(\lambda, 0)$ and $G(\lambda, 0)$. A more effective way to increase accuracy for larger values of λ is provided by entry (2) in Table 1. These expressions for H and W were obtained by using hydrodynamic results of Bungay and Brenner (1973) in Eqs. 24 and 25; they have been given in this form previously by Deen et al. (1985). The expressions for K_s and K_t are composites of asymptotic centerline results for small and for closely fitting spheres, and are accurate to within 10% for all radius ratios (Bungay and Brenner, 1973).

More rigorous analytical results for H and W are available for restricted ranges of λ. Brenner and Gaydos (1977) performed the radial integrations needed to determine K_d and K_c (Eqs. 9 and 10, with $E = 0$), using matched asymptotic expansions valid for small λ. Mavrovouniotis and Brenner (1986) have obtained analogous results for K_d for closely fitting ($\lambda \to 1$), eccentrically positioned spheres. Expressed in terms of H and W, these results are given as entries (3) and (4) in Table 1.

The behavior of the hindrance factors $H(\lambda)$ and $W(\lambda)$ for neutral spheres ($E = 0$) is shown in Figure 2. In addition to the results already mentioned, points shown at $\lambda = 0.5$ have been derived by Mitchell (1984) from values of $K^{-1}(0.5, \beta)$ and $G(0.5, \beta)$ calculated numerically by Lewellen (1982). For each of the methods of calculation represented in Figure 2, the more rapid decline of H than W with increasing λ indicates that diffusion is more sensitive to pore size than is convection. For a solute whose radius is only one-tenth that of the pore ($\lambda = 0.1$), the macroscopically observable diffusivity is already some 40% below the bulk solution value ($H \simeq 0.6$). At $\lambda = 0.9$, H is three orders of magnitude lower than W.

Figure 2 permits an assessment of the centerline approximation embodied in Eqs. 24 and 25. For small values of λ, the more exact diffusional hindrance factor derived by Brenner and Gay-

Table 1. Hydrodynamic Coefficients for Netural Spheres ($E = 0$) in Cylindrical Pores

Reference	H	W	Comments
(1) Anderson & Quinn (1974)	$\Phi(1 - 2.1044\lambda + 2.089\lambda^3 - 0.948\lambda^5)$	$\Phi(2 - \Phi)(1 - \frac{2}{3}\lambda^2 - 0.163\lambda^3)$	Centerline $0 \le \lambda < 0.4$
(2) Bungay & Brenner (1973)*	$\dfrac{6\pi\Phi}{K_t}$	$\dfrac{\Phi(2 - \Phi) K_s}{2K_t}$	Centerline $0 \le \lambda < 1$
	$\left(\dfrac{K_t}{K_s}\right) = \dfrac{9}{4}\pi^2\sqrt{2}(1 - \lambda)^{-5/2}\left[1 + \sum_{n=1}^{2}\left(\dfrac{a_n}{b_n}\right)(1 - \lambda)^n\right] + \sum_{n=0}^{4}\left(\dfrac{a_{n+3}}{b_{n+3}}\right)\lambda^n$		
(3) Brenner & Gaydos (1977)	$1 - \left(\dfrac{9}{8}\right)\lambda \ln \lambda^{-1} - 1.539\lambda + o(\lambda)$	$\Phi[1 + 2\lambda - 4.9\lambda^2 + o(\lambda^2)]$	Radial average $\lambda < \sim 0.1$
(4) Mavrovouniotis & Brenner (1986)	$0.984(1 - \lambda)^{9/2}$	—	Radial average $\lambda > \sim 0.9$

*The coefficients in K_t and K_s are
$a_1 = -73/60$; $a_2 = 77{,}293/50{,}400$; $a_3 = -22.5083$; $a_4 = -5.6117$; $a_5 = -0.3363$; $a_6 = -1.216$; $a_7 = 1.647$
$b_1 = 7/60$; $b_2 = -2{,}227/50{,}400$; $b_3 = 4.0180$; $b_4 = -3.9788$; $b_5 = -1.9215$; $b_6 = 4.392$; $b_7 = 5.006$

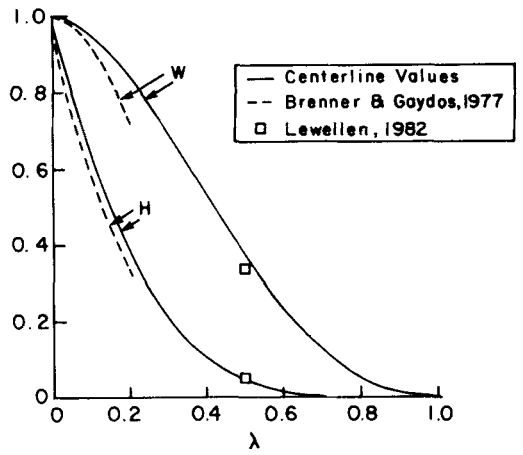

Figure 2. Hindrance factors for diffusion H and convection W of dilute solutions of neutral spheres in cylindrical pores.

See text for explanation of calculations

dos (1977) falls below the value of H obtained from the centerline approximation. Radial integration of K^{-1} lowers H in this case because small spheres close to the pore wall exhibit greater drag coefficients than those near the centerline (Brenner and Gaydos, 1977; Anderson and Quinn, 1974). At $\lambda = 0.1$, however, the centerline value of H is only 9% larger than the more exact result. By contrast, the result of Mavrovouniotis and Brenner (1986) for large λ (not distinguishable on the scale of Figure 2) exceeds the less exact centerline value of H; the ratio is 1.46 at $\lambda = 0.9$ and approaches 1.64 as $\lambda \to 1$. The exact $H(\lambda)$ and its centerline approximation must therefore cross at some intermediate value of λ. It is not surprising, then, that the value of $H(0.5)$ obtained from the results of Lewellen (1982) is indistinguishable from the centerline value. As with $H(\lambda)$, the centerline values of $W(\lambda)$ are remarkably close to the more exact results for small λ and for $\lambda = 0.5$. Similar agreement between centerline and integrated values of W was found by DuBois and Stoupel (1976), who evaluated the latter using experimental results for $G(\lambda, \beta)$.

Not shown in Figure 2 are certain other results obtained from various approximations to the off-axis behavior of K^{-1} and G. Anderson and Quinn (1974) integrated Eq. 15 numerically, using hydrodynamic approximations for small λ, and obtained values of H virtually indistinguishable from those of Brenner and Gaydos (1977). The numerical results of Lightfoot et al. (1976) for σ_f with $0 \le \lambda \le 0.2$ yield values of W between those of Brenner and Gaydos and the centerline approximation. Analytical expressions for σ_f from Curry (1974) and Anderson and Adamski (1983), using other off-axis approximations for G, give numerical results essentially equivalent to the centerline approximation.

The calculations in Figure 2 assume that long-range interactions between the solute and pore wall are absent ($E = 0$). If such interactions are repulsive (i.e., $E > 0$), there will be a bias toward solute positions near the centerline, and the centerline hydrodynamic approximation will be even more accurate than for $E = 0$. Only for attractive interactions ($E < 0$) is there likely to be a problem. One may conclude that the centerline approximation should be sufficiently accurate for most purposes.

Taylor dispersion

Radial variations in axial velocity, combined with radial diffusion, lead to deviations from the equilibrium form of the radial concentration profiles represented by Eq. 7. As described by Taylor (1953) and Aris (1956) for $\lambda \to 0$ and $E = 0$, this leads to axial dispersion greater than that provided by molecular diffusion alone. Brenner and Gaydos (1977) generalized the Taylor-Aris analysis to allow for $\lambda \neq 0$ and $E \neq 0$. In the present notation, Taylor dispersion may be included by replacing K_d in Eq. 8 with $K_d + K_v$, and replacing H with H^*:

$$H^* = \Phi(K_d + K_v) \tag{26}$$

The convective contribution to dispersion derived by Brenner and Gaydos, valid for $E = 0$ and small λ, may be expressed as:

$$\Phi K_v = \frac{\hat{Pe}^2}{48}[1 - 3.862\lambda + 14.40\lambda^2 + o(\lambda^2)] \tag{27}$$

$$\hat{Pe} = \frac{\langle V \rangle r_0}{D_\infty} \tag{28}$$

These results give an indication of the quantitative significance of Taylor dispersion in hindered transport. For $\lambda = 0.1$ and for $K_v/K_d > 0.1$ (i.e., >10% augmentation of molecular diffusion), it follows from Eqs. 27 and 28 and Table 1 that the radial Peclet number, $\hat{Pe}$, must exceed approximately 2. However, the axial Peclet number (Pe, Eq. 14) must then be quite large, because the analyses are restricted to long pores. Choosing as a minimum $L/r_0 = 10$, $Pe = 29$ for $\hat{Pe} = 2$ and $\lambda = 0.1$. For Pe this large, axial dispersion is insignificant relative to convection; indeed, Eq. 13 is within 1% of Eq. 18 provided only that $Pe > 5$. It may be concluded that, at least for small λ, the Taylor dispersion contribution represented by K_v will have a negligible effect on the solute flux, at any Peclet number. Although numerical results are not available, this situation seems unlikely to change for larger λ. Because of the factor W/H in Pe, which is of order unity for small λ but of order 10^3 for $\lambda = 0.9$, the ratio $Pe/\hat{Pe}$ increases sharply at large λ. Thus, for Taylor dispersion to significantly affect solute fluxes at large λ, the value of K_v would have to be several orders of magnitude greater than that in Eq. 27.

Electric fields and other long-range interactions

The numerical results for H and W discussed thus far include only steric and hydrodynamic interactions between the solute and pore wall. However, colloidal forces that contribute to E may also have large effects on these hindrance factors; examples include electrostatic and dispersion forces. If the continuous phase in the pore is an electrolyte solution, electrostatic interactions between a charged macrosolute and a charged pore wall will be partially screened. The additional length scale that arises is the Debye length, ℓ, which is a characteristic thickness of diffuse double layers adjacent to charged surfaces (Smith and Deen, 1983):

$$\ell = \left[\frac{F^2}{\epsilon RT}\sum_i (z_i^2 C_{i\infty})\right]^{-1/2} \tag{29}$$

where F is Faraday's constant, ϵ is the solvent dielectric permit-

tivity, and z_i and $C_{i\infty}$ are the valence and bulk solution concentration, respectively, of electrolyte species i. Electrostatic interactions will tend to be most prominent for small pores and/or low electrolyte concentrations, where ℓ becomes comparable to the pore radius.

Munch et al. (1979) modeled repulsive electrostatic interactions by simply adding ℓ to the solute radius, and subtracting it from the pore radius, in calculating λ. Malone and Anderson (1978) gave a more sophisticated yet still approximate treatment of the electrostatic and dispersion (van der Waals) contributions to $E(\beta)$, using expressions that had been derived previously for spheres interacting with flat plates. The electrostatic component of $E(\beta)$ for a spherical colloid in a cylindrical pore was later determined more precisely by Smith and Deen (1983). They obtained series representations of the electrical potential within the pore and membrane matrix by solution of the linearized Poisson-Boltzmann equation, and then calculated $E(\beta)$ from the change in free energy resulting from introduction of the colloid into the pore. Analytical expressions for $E(\beta)$ were derived for solid spheres having a constant surface potential or surface charge density, and for porous spheres having a given volumetric charge density.

The effects of electrostatic interactions on Φ, for solutes and pores of like charge, are illustrated in Figure 3. In these calculations Φ was evaluated from Eq. 11 (Smith and Deen, 1983). The partition coefficient is shown as a function of solution ionic strength, or of the ratio of pore radius to Debye length. For solid spheres of fixed surface charge density (curves marked S, Figure 3), Φ increases with ionic strength, eventually approaching the purely steric limit as $r_0/\ell \to \infty$. Of interest is that for the moderate charge densities chosen, appreciable effects of charge on Φ are predicted even for r_0/ℓ as large as 20. For highly porous spheres—a model sometimes used to represent randomly coiled polyelectrolytes—charge effects tend to be weaker (curves marked P, Figure 3). That is, distributing the same number of elementary charges throughout the sphere volume gives a weaker electrostatic interaction with the pore wall than if that same charge resided on the sphere surface. For both models, electrostatic effects at small r_0/ℓ are sufficient to exclude virtually all particles from the pore ($\Phi \to 0$).

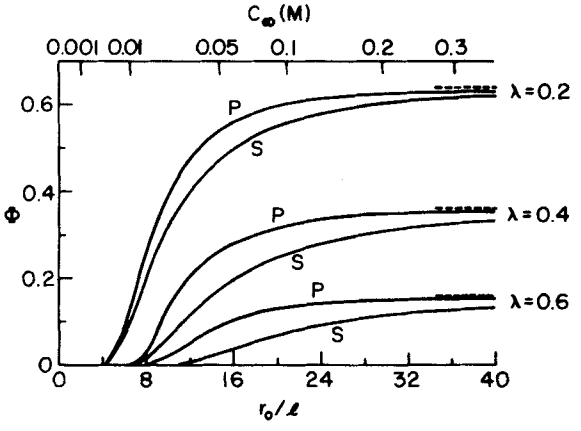

Figure 3. Partition coefficient Φ of charged spheres in cylindrical pores as a function of ionic strength C_∞ or of ratio of pore radius to Debye length r_0/ℓ.

S, solid spheres; P, highly porous spheres
Calculations assume a dilute solution of macrosolute in an aqueous univalent-univalent electrolyte at 37°C, with $r_0 = 200$ Å, $q_c = q_s = 10^{-2}$ C/m^2
To maintain equal particle charges at a given solute size, the volumetric charge density of the porous spheres was taken to be $3q_s/(\lambda r_0)$
From Figure 4, Smith and Deen (1983), with permission

For constant surface charge densities on the sphere, q_s, and pore wall, q_c, the electrostatic interaction energy was shown to contain terms proportional to q_s^2 and q_c^2, as well as to $q_s q_c$ (Smith and Deen, 1980, 1983). Thus, Φ is expected to deviate from the purely steric limit even when only one surface is charged. The terms involving q_s^2 and q_c^2 arise from the distortion of an electric double layer caused by introduction of a second, uncharged object (sphere or pore). Analogous quadratic forms were obtained for porous spheres or for constant potential boundary conditions (Smith and Deen, 1980, 1983). When both sphere and pore are charged, however, the cross term (e.g., $q_s q_c$) is usually dominant.

The electric charge effects just described arise in the absence of potential gradients imposed along the pore axis. Hindered particle motion in applied fields has received less attention. Keh and Anderson (1985) analyzed boundary effects on the electrophoretic motion of spheres, for the special case of thin double layers ($r_s/\ell \to \infty$). For spheres moving along the axis of a circular cylinder, or along the midplane of a parallel-plate channel, wall effects in electrophoresis were found to be much weaker than for translation of uncharged spheres.

Dispersion forces have usually been expressed in terms of Hamaker constants, and contributions to $E(\beta)$ estimated using results for spherical particles interacting with semiinfinite slabs (Malone and Anderson, 1978; Mitchell and Deen, 1984). When repulsive electrostatic forces are also present, the importance of these attractive forces may be minimal (Mitchell and Deen, 1984). However, the wide range of reported Hamaker constants, together with uncertainties in the proper form of interaction potential, makes generalizations hazardous. More research is clearly needed in the characterization of solute-pore wall interactions, especially attractive forces.

Other pore shapes

Other than the circular cylinder, fairly complete results are available only for the parallel plane or so-called "slit" geometry. For a channel of half-width h, the particle-to-pore size ratio is redefined as $\lambda = r_s/h$. The results analogous to Eqs. 15 and 16 (but with $E = 0$) are:

$$H = \int_0^{1-\lambda} K^{-1} d\beta \tag{30}$$

$$W = \frac{3}{2} \int_0^{1-\lambda} G(1 - \beta^2) d\beta \tag{31}$$

For $E \neq 0$, the term $\exp[-E/kT]$ should appear in both integrals.

The functions $K(\lambda, \beta)$ and $G(\lambda, \beta)$ are different for slits than for cylinders. Ganatos et al. (1980) used a strong interaction theory and a collocation method to obtain numerical values of these functions covering a wide range of λ and β. These rather complete results were used by Weinbaum (1981) to evaluate the integrals in Eqs. 30 and 31, thereby making available "exact" values of $H(\lambda)$ and $W(\lambda)$ for neutral spheres in slit pores. (See Appendix, note 3, on Weinbaum's results.)

Analytical expressions for slits are limited. Using centerline approximations for K and G (analogous to Eqs. 24 and 25):

$$H \simeq \Phi[1 - 1.004\lambda + 0.418\lambda^3 + 0.21\lambda^4 - 0.169\lambda^5 + 0(\lambda^6)] \quad (32)$$

$$W \simeq \frac{\Phi}{2}(3 - \Phi^2)\left[1 - \frac{\lambda^2}{3} + 0(\lambda^3)\right] \quad (33)$$

where the partition coefficient for $E = 0$ is given by

$$\Phi = 1 - \lambda \quad (34)$$

The terms in square brackets in Eqs. 32 and 33 represent $K^{-1}(\lambda, 0)$ and $G(\lambda, 0)$, respectively, from Faxén, as cited by Happel and Brenner (1983, pp. 67, 327).

Figure 4 compares the exact numerical results of Weinbaum (1981) for slits with the centerline approximations represented by Eqs. 32 and 33. Although H and W decline somewhat less rapidly with increasing λ in slits than in cylindrical pores, their behavior in the two geometries is qualitatively similar. However, the centerline approximations in slits consistently overestimate H and W, by 8% and 1%, respectively at $\lambda = 0.1$, and 14% and 7% at $\lambda = 0.5$. An approximate analytical expression for W from Anderson and Adamski (1983), obtained by partial inclusion of radial variations in G, is numerically indistinguishable from the centerline approximation, Eq. 33. Values of the reflection coefficient reported by Curry (1974), who used another approximation to the off-axis behavior of $G(\lambda, \beta)$, are less than any of those for σ_f, but are very close to those obtained for σ_0 in this geometry by Anderson (1981).

Pores of rhomboidal cross section are of particular interest experimentally because the pores of track-etched mica membranes are rhomboids with an acute angle of 60°. Partition coefficients for spherical molecules in this geometry have been determined by Glandt (1981b). Although the hydraulic permeability L_p for rhomboidal pores is known (Idol and Anderson, 1986), other hydrodynamic results needed for evaluation of H and W are not, thereby motivating efforts to define equivalent circular cylinders. Possibilities include a cylinder with the same cross-sectional area, r_a (Malone and Anderson, 1978; Idol and Anderson, 1986); a cylinder with the same partition coefficient, r_p; a cylinder with the same product of partition coefficient and cross-sectional area (Glandt, 1981b); and the largest cylinder that will fit within the rhombus, r_c (Malone and Anderson, 1978). The partition coefficient for a rhombic pore is lower than that of a circular pore of the same cross-sectional area (i.e., $r_p < r_a$). It can be shown from geometric arguments, however, that $r_p = r_c$; that is, the radius of an inscribed circle, when used in Eq. 12, gives the correct partition coefficient for a rhombus. Also, $r_c = 0.825\ r_a$ for a 60° rhombus (Malone and Anderson, 1978). It is expected that use of r_a in the formulas for cylinders will slightly overestimate H and W (because Φ is too high), while use of r_c will slightly underestimate them (because K^{-1} and G are too low). These two approaches are compared by Malone and Anderson.

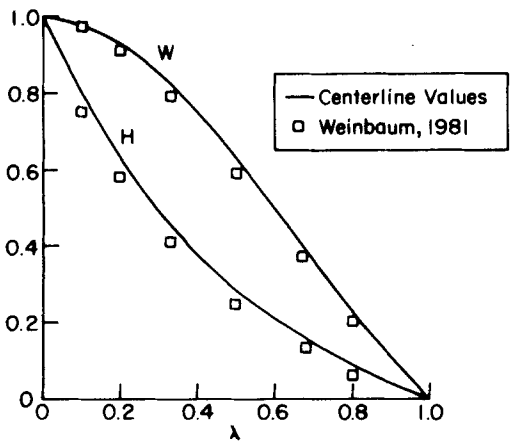

Figure 4. Hindrance factors for diffusion H and convection W of dilute solutions of neutral spheres in slit pores.
See text for explanation of calculations

Partition coefficients have been determined also for pores of rectangular or elliptical cross section (Anderson 1981; Giddings et al., 1968), for spherical cavities (Glandt, 1981a; Giddings et al., 1968), and for various regular polygons (Glandt, 1981b).

Pore entrance and exit effects on osmotic flow were the focus of a recent study by Yan et al. (1986). They matched separate solutions for the pore entrance, interior, and exit to estimate corrections to L_p and σ_0 for short pores ($L \sim r_0$), at various values of λ. With regard to pores of nonuniform cross section, Levitt (1975b) attempted to generalize his analysis for uniform pores by including axial variations in pore radius, assuming in his numerical examples that K and G could be evaluated based on the local value of the radius. Smith (1986) modeled pores with periodic constrictions by applying the Renkin equation for H to unit cells of alternating length and radius. For porous media consisting of random arrays of fibers, analyses are available to estimate Φ (Ogston, 1958; Fanti and Glandt, 1986) from the solute radius, fiber radius, and the volume fraction of fibers. Until recently, the available results for transport coefficients in fibrous media (Ogston et al., 1973; Curry and Michel, 1980) have neglected all hydrodynamic interactions between solutes and fibers. With regard to hydrodynamic interactions between a diffusing particle and a semidilute polymer solution (Cukier, 1984) or polymer gel (Altenberger and Tirrell, 1984), progress has been made by treating the polymer solution or gel as an effective medium characterized by a Brinkman screening length. The extension of hydrodynamic models of hindered transport to more complex geometries represents an opportunity for further research.

Nonspherical solutes

Giddings et al. (1968) presented a general formulation for the partitioning of rigid particles of arbitrary shape, with specific results given for thin rods, ellipsoids of revolution, and capsule-shaped molecules (cylinders with hemispherical end caps). Results for various molecular and pore shapes were well correlated using a mean projected molecular dimension. Baltus and Anderson (1984) used this finding to relate the Stokes-Einstein radius to the partitioning behavior of ellipsoidal molecules. Relative to either prolate or oblate ellipsoids of identical Φ, spheres were found to have the smallest value of D_∞ (largest r_s). Equivalently, for a given r_s, spheres have the maximum Φ. To the extent that

the hindrance coefficients for ellipsoids are controlled by partitioning, this would result in smaller values of H and W at a given λ for ellipsoids than for spheres.

Anderson (1981) extended the analysis of Anderson and Malone (1974) to obtain osmotic reflection coefficients for rigid, axisymmetric solutes. Interestingly, numerical results obtained for capsules in cylindrical pores support the general application of Eq. 23, with Φ calculated as described by Anderson (1981) or Giddings et al. (1968) for molecules of varying eccentricity. A formulation of H and W for nonspherical molecules in cylindrical pores was described by Anderson and Quinn (1974), and a much more general treatment for rigid particles and pores of arbitrary shape was given by Brenner and Gaydos (1977). Unfortunately, limitations of existing hydrodynamic data have precluded the evaluation of H and W even for relatively simple, axisymmetric molecules such as ellipsoids. An approximate treatment of convection of thin rigid rods in parallel plate channels was reported by DiMarzio and Guttman (1970), but that analysis neglects hydrodynamic retardation.

Effects of solute concentration

The results discussed thus far neglect solute-solute interactions, and therefore should be accurate only for very dilute solutions. One effect of finite concentrations is to cause the radial concentration profiles to deviate from the simple Boltzmann distribution given by Eq. 7. A second effect is to introduce hydrodynamic interactions among solutes, thereby modifying K and G. The first (thermodynamic) effect has now been characterized fairly well, while the second (hydrodynamic) has not.

Glandt (1980) was the first to report the effects of concentration on particle density profiles in pores, by drawing analogies to certain statistical treatments of binary solutions. Equilibrium concentration profiles were expressed as virial-type expansions in powers of the external bulk concentration C_∞:

$$C(\beta) = C_\infty \exp\left[-E(\beta)/kT\right]\left[1 + \sum_{n=1}^{\infty} Y_n(\beta) C_\infty^n\right] \qquad (35)$$

Expressions for the coefficients Y_n were obtained in terms of configurational integrals involving the solute-pore and solute-solute interaction potentials. Numerical results for Y_1 and Y_2 were presented for purely steric (hard sphere-hard wall) interactions. The major finding was that shielding of solute-solute interactions by the pore wall induces solute accumulation near the wall, even in the absence of any attractive forces.

Values of Φ at finite concentration have been computed by replacing the Boltzmann factor in Eq. 11 by radial profiles in the form of Eq. 35. Results for Φ based on purely steric interactions, employing both Y_1 and Y_2, were presented by Glandt (1981a) and Anderson and Brannon (1981) for both cylindrical pores and slits. Electrostatic interactions were discussed briefly by Anderson and Brannon and in more detail by Mitchell and Deen (1984). Some representative results for cylindrical pores, including terms only up to Y_1, are shown in Figure 5. $\Phi(\lambda)$ is plotted with the volume fraction of solute in bulk solution f as a parameter. For uncharged solutes and pores, the dilute solution limit (dashed curve, $f = 0$) is from Eq. 12. Whether solutes and pores are uncharged (dashed curves) or of like charge (solid-line curves), solute-solute repulsion promotes increased concentrations near the periphery of the pores, thereby causing Φ to increase with f. For the uncharged case and $f \neq 0$, including the

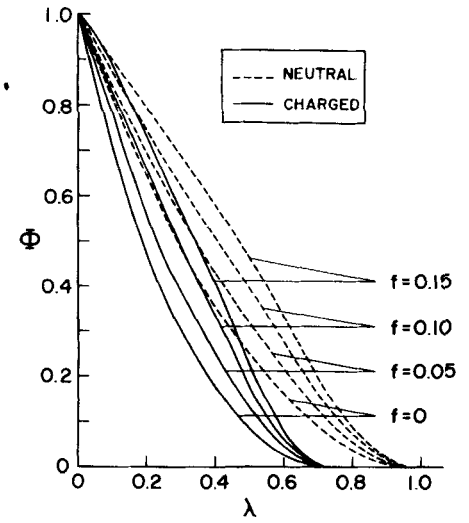

Figure 5. Effect of the volume fraction of solute in bulk solution f on the partition coefficient Φ for spherical solutes in cylindrical pores.

Calculations for charged solutes and pores assume a 0.05 M aqueous solution of a univalent-univalent electrolyte at 25°C, with r_0 = 200 Å, $q_c - q_s = 10^{-2}$ C/m²
From Figure 2, Mitchell and Deen (1986), with permission

Y_2 term elevates Φ for $\lambda > \sim 0.4$, and lowers Φ for $\lambda < \sim 0.4$, relative to the curves shown in Figure 5 (Glandt, 1981a).

The effects of solute concentration on partitioning have been reported also for spherical cavities (Glandt, 1981a) and for pores of rhombic or regular polygonal cross section (Glandt, 1981b), based on steric interactions. In addition, Post and Glandt (1985) examined concentration effects in the presence of short-range solute-pore attractions. They employed an "adhesive surface" potential, a limiting form of the square well potential in which the well becomes infinitely deep and infinitesimally narrow. In this model an adsorbed monolayer coexists with free solute within the pore. Results were reported including coefficients up to Y_2.

Analyses of the effects of concentration on the reflection coefficients σ_f (Anderson and Adamski, 1983; Mitchell and Deen, 1984) and σ_0 (Adamski and Anderson, 1983; Anderson and Adamski, 1983) generally predict decreases in either quantity with increases in bulk concentration, as would be expected from the behavior of Φ. However, lacking to date has been a detailed evaluation of the effects of solute-solute hydrodynamic interactions on these or other transport coefficients. Adamski and Anderson (1983) estimated the contributions of solute interactions to the viscous stresses needed to calculate σ_0, and concluded that they were negligible. In general, one would expect that if solute-wall hydrodynamic interactions are much more important than those between solutes, the dominant effects of C_∞ on H and W would come from the altered equilibrium distribution of solute. This is the situation assumed in the analyses of the concentration dependence of σ_f (Anderson and Adamski, 1983; Mitchell and Deen, 1984). For the special case of spheres evenly spaced along the centerline of a cylindrical tube, effects on K are not noticeable until the sphere spacing is roughly one tube radius, and changes in G are <2% even for spheres touching (Wang and Skalak, 1969). These results could serve as rough guidelines for large λ, where particles must travel in sin-

gle file. A criterion for weak hydrodynamic interactions among small spheres, suggested by Happel and Brenner (1983, p. 361), is that the surface area of the particles be small compared to that of the container walls. This will be true if

$$f\Phi \ll \lambda \tag{36}$$

where $f\Phi$ is the volume fraction of particles within the pore. Further efforts to characterize the effects of solute-solute hydrodynamic interactions on H and W are clearly needed. Another factor that should not be neglected in refining solute flux equations for concentrated solutions is the contribution of the solute flux to volume flow (Lightfoot et al., 1976).

Experiments Using Rigid Solutes in Model Membranes

Effects of size on diffusion

Track-etched membranes provide a means to test the predictions of hindered transport theory in pores that are straight and of uniform cross section, without the need to invoke correction factors such as tortuosity. This review of experimental results therefore focuses almost exclusively on these model membranes. One of the earlier and more extensive tests of the effects of molecular and pore size was provided by Beck and Schultz (1972), who examined diffusion of urea, several carbohydrates, and ribonuclease (a small protein) in track-etched mica membranes having pore radii of 45–300 Å. The pore number densities of these membranes were determined by electron microscopy, and pore radii from water flow, treating the pore cross section as elliptical. Diffusion data from this study are plotted in Figure 6, where D is the apparent diffusivity based on the external concentration difference (i.e., $D \equiv HD_\infty$). The curve shown is the prediction of $H(\lambda)$ from Eq. 24 (centerline approximation). Despite some scatter in the data, the rapid decline in D/D_∞ with increasing λ generally conforms quite well to that predicted by the theory. One limitation of this study is that, unlike most track-etched mica preparations employed subsequently, the membranes used exhibited a distribution of pore sizes.

A more limited study using track-etched polycarbonate membranes of about 150 Å pore radius was performed by Van Brug-

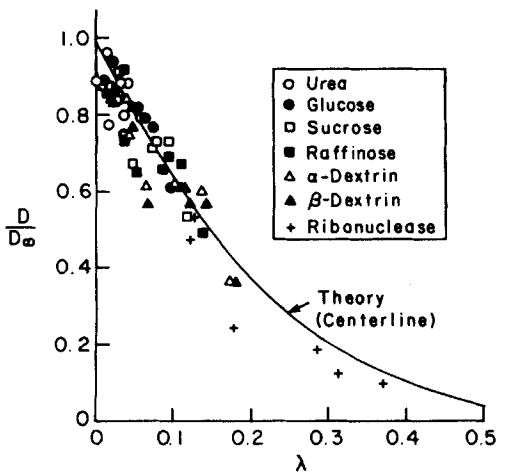

Figure 6. Hindered diffusion data for compact solutes in track-etched mica membranes.
Plotted from tabular data given by Beck and Schultz (1972)

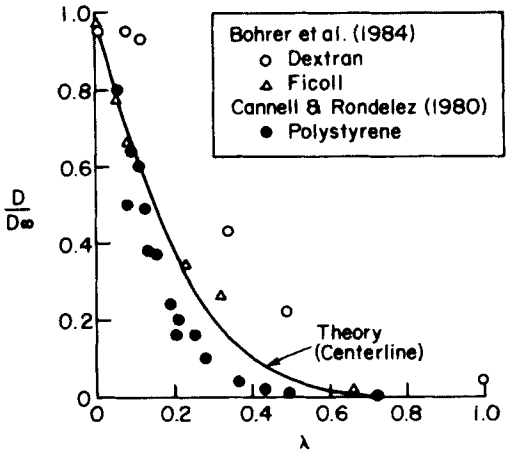

Figure 7. Hindered diffusion data for polymers in track-etched polycarbonate membranes.

gen et al. (1974). Membranes were characterized by electron microscopy, water flow, and diffusion of tritiated water. Three small solutes (mannitol, sucrose, and maltotriose, λ = 0.03–0.04) exhibited values of D/D_∞ very close to the theoretical predictions for neutral spheres. (See Appendix, note 4, regarding some D/D_∞ values.) For inulin, a polymer of fructose with molecular weight about 5,000, D/D_∞ at $\lambda = 0.10$ was only about two-thirds of that expected for a solid sphere. However, it is doubtful that inulin is well represented as a rigid particle, and a low value of D/D_∞ is in fact consistent with expectations for flexible polymers (see below).

A relatively rigid and uncharged polymer that has been studied is ficoll, a crosslinked copolymer of sucrose and epichlorohydrin. Measurements of intrinsic viscosity and partial specific volume, interpreted using a model for rigid ellipsoids, yield an axial ratio for ficoll near unity (Bohrer et al., 1979). Ficoll diffusion in track-etched polycarbonate membranes was examined by Deen et al. (1981) for $0.2 < \lambda < 0.5$, and by Bohrer et al. (1984) for $0 < \lambda < 0.7$. Qualitatively similar results were obtained in the two studies, but the work of Bohrer et al. employed improved methodology. As shown in Figure 7, values of D/D_∞ reported by Bohrer et al. for ficoll are in excellent agreement with Eq. 24.

Another test of hindered diffusion of uncharged particles was provided by Baltus and Anderson (1983), who studied asphaltene diffusion in track-etched mica membranes. Asphaltenes, extracted from petroleum residuals, are complex multimolecular aggregates of uncertain shape and covering a range of sizes. Five fractions obtained by gel permeation chromatography were studied, with Stokes-Einstein radii of 26–153 Å. Measured values of D/D_∞ were in excellent agreement with Eq. 24 for $\lambda < 0.25$ (using r_a as the pore radius). Agreement was less satisfactory for larger size ratios, but could be improved by an empirical adjustment of Φ, based on a comparison of the gel chromatographic behavior of asphaltenes and polystyrene (Baltus and Anderson, 1983).

Globular proteins such as bovine serum albumin (BSA, $r_s \simeq$ 36 Å) are usually regarded as having the hydrodynamic characteristics of solid particles (Tanford, 1961). Wong and Quinn (1976) studied hindered diffusion of BSA in track-etched mica membranes (in 0.05 M phosphate buffer at pH 8), and found

D/D_∞ at $\lambda = 0.19$ to be only about one-half that predicted for neutral spheres. It was argued that this discrepancy did not result from effects of electrical charge, because similar values of D/D_∞ were obtained when the ionic strength of the solution was increased tenfold by addition of KCl. One possible contributing factor is that BSA is better represented as a prolate ellipsoid of axial ratio 3.4 (Wright and Thompson, 1975), for which Φ should be lower than for a sphere having the same Stokes-Einstein radius (Baltus and Anderson, 1984). More important, recent data from the same laboratory seem to cast doubt on the conclusion that charge effects played little or no role. Rodilosso (1984) estimated Φ for BSA in track-etched mica membranes, using electrical conductance and tracer (THO) diffusion measurements. In computing Φ, adsorbed BSA was excluded. For the conditions most closely resembling those of the earlier diffusion study (dilute solution of BSA at pH 8.5 and 0.2 M ionic strength, with $\lambda \simeq 0.2$), Φ was found to be at least an order of magnitude lower than that expected from Eq. 12 for neutral spheres. As discussed by Rodilosso, these partitioning results are best explained by electrostatic repulsion between BSA molecules in solution and the BSA-coated pore wall. It appears then that the BSA diffusion data of Wong and Quinn (1976) may not provide a good test of predictions for neutral solutes.

Effects of charge on diffusion

Malone and Anderson (1978) examined the effects of electrostatic interactions on hindered diffusion using latex particles ($r_s = 455$ Å) in track-etched mica membranes, with pore radius and ionic strength being the principal variables. Although particle and pore charges were not measured, evidence was cited that both surfaces carried net negative charges. As expected, D/D_∞ declined sharply with increases in λ at any given ionic strength. D/D_∞ also declined as ionic strength was reduced (ℓ increased), at any given λ, as expected for repulsive electrostatic interactions. An approximate theoretical treatment of size and charge effects (Malone and Anderson, 1978) was able to explain these main trends, although use of these data in a more quantitative test of the theory is largely precluded by the absence of charge measurements.

In a more recent study of the effects of charge on hindered diffusion, Deen and Smith (1982) attempted to measure all required input parameters, including solute and pore charge. The molecular charge of ficoll sulfate and the surface charge density of polycarbonate track-etched membranes (both negative) were determined from measurements of electrophoretic mobility and streaming potential, respectively. Pore size and number density were calculated from measurements of water flow and diffusion of a small solute (glucose), and D_∞ for ficoll sulfate fractions was measured using large-pore membranes. As ionic strength (KCl concentration) was increased from 0.005 to 0.1 M, D_∞ for ficoll sulfate was unchanged, whereas D/D_∞ in small-pore membranes increased by as much as a factor of 14. Theoretical calculations were based on Eq. 24, with ficoll treated as a charged, porous sphere for determination of Φ, and as a solid sphere for estimation of $K^{-1}(\lambda, 0)$. These predictions were generally in good quantitative agreement with the data.

Convection and osmosis

Measurements of σ_f for dilute solutions of BSA have been reported by Munch et al. (1979) for track-etched mica membranes, and by Mitchell and Deen (1986) for track-etched polycarbonate at pH 6.7–6.8. Changes in r_0 resulting from BSA adsorption were estimated from serial measurements of L_p. In both cases the values of σ_f exceeded those predicted for neutral spheres. This can be explained in part by repulsive electrostatic interactions between BSA and the pore wall, as demonstrated clearly by the inverse dependence of σ_f on ionic strength observed by Munch et al. However, even when considerable care was taken to correct the theoretical predictions for charge effects, Mitchell and Deen found that σ_f still exceeded the predicted value by as much as a factor of 2 for $\lambda = 0.1 - 0.2$. The ellipsoidal shape of BSA may contribute to the remaining discrepancy.

Polymer adsorption to the pore walls complicates the interpretation of hindered transport experiments, especially in the presence of transmembrane volume flow. Exposure of track-etched polycarbonate or mica membranes to BSA leads quickly to an irreversible decrease in pore radius roughly comparable to that expected for an adsorbed monolayer (Wong and Quinn, 1976; Schultz et al., 1979; Munch et al., 1979; Yavorsky, 1981; Rodilosso, 1984; Mitchell and Deen, 1986). The most precise measurements with BSA in mica pores suggest that the long axis of the molecule is parallel to the surface (Yavorsky, 1981; Rodilosso, 1984). Despite preequilibrating their mica membranes with BSA solutions, Munch et al. noted further transient decreases in hydraulic permeability during ultrafiltration, which were only partially reversed by subsequent flushing with protein-free solutions. In preequilibrated polycarbonate membranes of similar pore radius (~300 Å), Mitchell and Deen (1986) found r_0 (from water flow) and σ_f for BSA to remain constant over several hours. However, when initially $r_0 \simeq 150$ Å, marked transient decreases in r_0 and increases in σ_f were observed during ultrafiltration of BSA, which could not be reversed with protein-free solutions. Yavorsky (1981) observed a further decrease in the hydraulic permeability of BSA-coated mica membranes at wall shear stresses above 50 Pa, and attributed this change to shear-induced denaturation of the adsorbed protein. Of interest is that the wall shear stresses reported by Mitchell and Deen exceeded this threshold in the smaller pores mentioned above, but not in the larger pores.

Because of polymer adsorption, pore radii inferred from water flow or diffusion of small tracers may underestimate hindrances to the movement of large solutes. Mitchell and Deen (1986) found that after exposure of a membrane to concentrated solutions of ficoll or BSA, the dilute solution σ_f tended to increase much more than would have been expected from the decrease in r_0 inferred from water flow. They speculated that adsorbed polymer may have permitted some water flow in the annular region near the pore wall, while excluding macromolecules. The differing effects of adsorbed polymer on momentum and mass transfer were studied more directly by Idol and Anderson (1986). By varying ionic strength, they altered the configuration of linear polyelectrolytes adsorbed to the pores of mica membranes. The hydraulic permeability was found to be reduced more by expansion of the adsorbed polymers (reduction in ionic strength) than was diffusion of a small, neutral solute (thiourea). Hindered transport of macrosolutes was not examined, however.

Additional rigid colloids for which σ_f data are available in track-etched membranes are tobacco mosaic virus (TMV) and polystyrene latex particles (Long et al., 1981). TMV resembles a long rigid rod; the number-average length of the fragments

studied by Long et al. yields an axial ratio of about 15. The values of σ_f measured for TMV significantly exceeded those predicted for spheres of the same volume, and were in fairly good agreement with calculations of σ_0 using Eq. 23, with Φ evaluated for capsule-shaped molecules of the appropriate eccentricity. For latex particles, σ_f was in good agreement with the theory for neutral spheres at $\lambda \simeq 0.2$, but significantly exceeded predictions for $\lambda \sim 0.5$–0.6; however, transient decreases in apparent pore radius during latex ultrafiltration limit any conclusions from these data.

Schultz et al. (1979) measured σ_0 for BSA and bovine γ-globulin in track-etched polycarbonate membranes. The results for these globular proteins tended to scatter about the theoretical curve for dilute solutions of neutral spheres. It should be noted that because the protein concentrations used were 8–10% by weight, the measured values of σ_0 would tend to be lower than those at infinite dilution (Adamski and Anderson, 1983). At least in the case of BSA, electrostatic interactions with the membrane (including adsorbed protein) would be expected to elevate σ_0, thereby tending to compensate for the concentration effect.

Effects of concentration

Mitchell and Deen (1986) examined the effects of solute concentration on σ_f using two solutes that appear to behave as rigid particles, BSA and ficoll. Ultrafiltration experiments were performed at solute volume fractions f of 0.001 and 0.033–0.080 in track-etched polycarbonate membranes of varying pore radii, characterized by water flow and scanning electron microscopy. For all membrane-solute combinations studied, σ_f decreased with increasing concentration. The decreases in σ_f were in reasonable quantitative agreement with theoretical expectations for neutral (ficoll) or charged (BSA) spheres, assuming partitioning to be the dominant factor controlling changes in σ_f. Consistent with this interpretation are the partitioning data of Brannon and Anderson (1982) for BSA in controlled-pore glass (pH 8). They found Φ to increase with increasing f, in reasonable accord with predictions based on Eq. 35. Rodilosso (1984) found Φ for BSA in mica membranes to increase with f when net intermolecular forces were repulsive (high pH), and to decrease with f when these forces were attractive (low pH), again in qualitative agreement with predictions.

Hindered Transport of Flexible Polymers

Polymers which exist in solution as flexible coils have a number of characteristics that may lead to distinctive behavior in transport through small pores. Dimensions assigned to such molecules are of course only statistical averages of the many configurations achieved by random motion of chain segments. Random variations in molecular shape may permit passage through pores having radii considerably smaller than average molecular dimensions such as the Stokes-Einstein radius r_s or radius of gyration r_g. Superimposed on these random variations may be deformations induced by flow. When polymer concentrations are large enough to cause chains to interact with one another, the average overall dimensions of the chains are affected and entanglements begin to occur. Only recently have these phenomena received much attention in the context of hindered transport. This section reviews work to date in this area, both theoretical and experimental.

Diffusion

Representative data on the diffusion of polymers in track-etched polycarbonate membranes are shown in Figure 7, in comparison with theoretical predictions for neutral spheres. As already noted, the cross-linked polymer ficoll in water behaves as a solid sphere (Bohrer et al., 1984). However, other polymers that more closely resemble random coils differ significantly from ficoll and from one another. Polystyrene in ethyl acetate exhibits values of D/D_∞ lower than those expected for a solid sphere of the same Stokes-Einstein radius (Cannell and Rondelez, 1980) whereas D/D_∞ for dextran in water tends to be much higher (Deen et al., 1981; Bohrer et al., 1984). Results for polystyrene in tetrahydrofuran (Kathawalla and Anderson, 1986) are qualitatively similar to those for polystyrene shown in Figure 7.

The overall diffusion coefficients shown in Figure 7 reflect both partitioning and hydrodynamic hindrances. The partitioning of random-flight polymer chains between bulk solution and pores of various shapes was analyzed by Casassa (1967), using a mathematical analogy to transient heat conduction. The analytical results obtained are valid in the limit of an infinite number of chain segments of vanishingly small length. Davidson et al. (1987) used Monte Carlo simulations to confirm the limiting results of Casassa and to examine the effects of finite segment number and length. In both studies the measure of polymer size used was the radius of gyration r_g. Based on these results, and taking into account that $r_s \simeq 0.7\ r_g$ (Tanford, 1961, p. 345), it may be concluded that for a given value of λ, Φ for a linear, random coil polymer should be lower than that of a solid sphere.

Davidson and Deen (1987) modeled the hydrodynamic hindrances by treating the polymer coil as a porous body. The equation of Brinkman (1947) in axisymmetric form was used to define the flow, with spatial variations in the hydraulic permeability of the coil being related to segment densities obtained from Monte Carlo simulations. Parameters for a given polymer could be estimated using bulk solution data. The magnitudes of $K^{-1}(\lambda, 0)$ and $G(\lambda, 0)$ were found to be similar to those of solid spheres for small λ, but larger for $\lambda > 0.5$, indicating less hydrodynamic resistance to movement of the coils in this size range. However, the hydrodynamic differences were generally calculated to be insufficient to offset the lower values of Φ for random coils. Only for λ approaching or exceeding unity were H and W for random coils greater than for solid spheres. The predicted values of H were quite similar to the experimental results for polystyrene shown in Figure 7.

The fact that entropic and hydrodynamic considerations for neutral, random coils lead to values of H lower than those for solid spheres suggests that the elevated values of D/D_∞ for dextran result from some other factor. One possibility is the presence of weak attractions between dextran and the pore wall. Monte Carlo simulations based on an approximate treatment of polymer segment-pore wall attractions indicate that Φ may be increased several-fold at intermediate values of λ with attractive energies per segment of only 0.2–0.3 kT. (Davidson et al., 1987).

Other theoretical studies of the partitioning of polymers include that of Casassa and Tagami (1969), who extended the earlier work of Casassa to star-branched, random flight chains. The scaling analysis of Daoud and de Gennes (1977) considered not only ideal chains (i.e., polymers in theta solvents) but also good solvents. The trends for ideal chains are similar to those

found by Casassa (1967), but the lack of numerical coefficients in the scaling results precludes quantitative comparisons. Aubert and Tirrell (1982) used a linear elastic dumbbell model to obtain partition coefficients for polymer chains in pores of various shapes. Their results much more closely resemble those of Giddings et al. (1968) for a rigid rod than those of Casassa (1967).

The special case of diffusion of highly deformed polymers through pores has been considered in a scaling analysis by Brochard and de Gennes (1977). When combined with the partitioning results of Daoud and de Gennes (1977), this analysis (for good solvents) suggests that $H = a(\lambda^*)^{-2/3} \exp[-(\lambda^*)^{5/3}]$ for large λ. The dimensionless size λ^* has been interpreted variously as (roughly) the ratio of polymer end-to-end distance (Flory radius) to pore diameter (Daoud and de Gennes, 1977; Brochard and de Gennes, 1977), λ (Guillot et al., 1985), or $b\lambda$, where b is an adjustable constant (Cannell and Rondelez, 1980). The prefactor a was also reported to depend on λ^*, in some manner weaker than the exponential term (Daoud and de Gennes, 1977), although this seems to have been ignored in later applications (Guillot et al., 1985; Cannell and Rondelez, 1980).

Another recent model for diffusion of neutral polymers in fine pores is that of Adolf and Tirrell (1986). Gradient theory, a formulation that has been used to describe continuous variations in fluid properties near interfaces, was used to compute radial distributions of polymer segments in pores. This information was combined with solid-sphere hydrodynamic resistances to obtain predictions for D/D_∞. The principal parameter arising from gradient theory was a length scale I characteristic of fluid inhomogeneities adjacent to the interface (pore wall). The value of I required to fit viscosity or diffusion data for polymers in pores was about 20 μm (Adolf and Tirrell). The difficulty in predicting I *a priori* would seem to limit the utility of this approach. (For I and the elastic dumbbell model, see Appendix, note 5.)

Regarding effects of charge on flexible polymers, diffusion of dextran sulfate in track-etched polycarbonate membranes was examined by Deen and Smith (1982). As with ficoll sulfate, increases in ionic strength markedly elevated D/D_∞ for dextran sulfate. However, unlike ficoll sulfate, there was evidence from D_∞ and intrinsic viscosity data that dextran sulfate coils contracted when ionic strength was increased. Thus, conformational changes resulting from improved screening of intramolecular repulsions contributed to the behavior of D/D_∞ for dextran sulfate.

Convection at moderate flows

Several studies provide ultrafiltration data for flexible polymers in track-etched membranes at solvent flow rates that should be low enough for flow-induced deformation of the polymers to be negligible. Zeman and Wales (1981) and Long et al. (1981) both reported results for dextran in track-etched polycarbonate membranes that seem to be in good agreement with the predictions of W or σ_f for neutral spheres. Using similar membranes, Mitchell and Deen (1986) found σ_f for dextran to exceed that for solid spheres. These seemingly divergent findings may be reconciled in part by noting differences in the estimation of molecular and pore size. By using the manufacturer's nominal pore radii, Zeman and Wales may have underestimated r_0. This possibility is suggested by frequent reports of measured values of r_0 exceeding nominal values (Mitchell and Deen, 1986; Long et al., 1981; Bohrer et al., 1984; Deen and Smith, 1982). Long et al. plotted their data using a molecular radius derived from intrinsic viscosity data, which should exceed r_s for dextran by about 10% (M.G. Davidson, personal communication). If these tendencies to overestimate λ are taken into account, the results of Zeman and Wales and Long et al. appear somewhat more consistent with those of Mitchell and Deen (1986).

Differences among the ultrafiltration results aside, the finding that σ_f for dextran is greater than or equal to that for a solid sphere is difficult to reconcile with other results. The high values of D/D_∞ for dextran, Figure 7, suggest that σ_f should be lower than that for solid spheres of the same Stokes-Einstein radius, not higher. Qualitatively similar to the results for D/D_∞ is the enhancement of dextran transport relative to that of ficoll during ultrafiltration in blood capillaries of the kidney (Bohrer et al., 1979). Also inconsistent with the findings for σ_f are the relatively low values of σ_0 measured for dextrans in track-etched polycarbonate membranes (Schultz et al., 1979); however, it should be noted that these values of σ_0 may be substantially lower than dilute solution values (Adamski and Anderson, 1983).

Ultrafiltration studies using other linear polymers also do not conform to a single pattern. For polystyrene in a mixed carbon tetrachloride-methanol solvent, at low flows, Long and Anderson (1984) found σ_f in track-etched mica membranes to be less than or equal to that expected for neutral, solid spheres. Based on the depressed D/D_∞ for polystyrene in ethyl acetate (Cannell and Rondelez, 1980) and tetrahydrofuran (Kathawalla and Anderson, 1986), elevations in σ_f might have been expected. Such elevations in σ_f seem to have been observed by Zeman and Wales (1981) for polyethylene oxide, if their data are plotted in terms of Stokes-Einstein radius (assuming $r_s \simeq 0.7\, r_g$).

Flow-induced deformation

The ultrafiltration data already discussed were obtained at solvent flow rates that should be sufficiently small to avoid flow-induced deformation of the test polymers. A criterion for neglecting such deformations is (Long and Anderson, 1984)

$$\dot{\gamma}\tau \ll 1 \tag{37}$$

where $\dot{\gamma}$ is a characteristic rate of strain in the solvent and τ is a time constant for the slowest relaxation mode of the polymer chain. For the elongational flow near the entrance of a pore, a suitable characteristic rate of strain is $\langle V \rangle / r_0$. For dilute solutions of linear polymers, τ may be estimated as (Ferry, 1980):

$$\tau \simeq \frac{\eta M[\eta]}{2RT} \tag{38}$$

where $[\eta]$ is the intrinsic viscosity of the polymer (zero shear limit) and M is its molecular weight.

In one set of experiments by Long and Anderson (1984), with $\lambda < 1$, σ_f was found to decrease with increasing $\dot{\gamma}\tau$ when $\dot{\gamma}\tau$ exceeded ~0.05. More dramatic effects of flow were demonstrated in a second set of experiments, with $\lambda > 1$. In this case σ_f declined from near unity at low flows to ~0.2 at the highest flow rates examined. Of particular interest is that the results for $\lambda > 1$ were insensitive to molecular weight and pore radius, the controlling variable being the volume flow per pore, Q. The results in this range of λ were well correlated by a dimensionless vari-

able $s = \eta Q/kT$, with $\sigma_f = 0.5$ at $s = 0.27$. These findings are partly in accord with a scaling analysis (Daoudi and Brochard, 1978), which correctly predicts s to be the only important variable. However, the scaling analysis suggests a sharp transition from $\sigma_f = 1$ to $\sigma_f = 0$ at $s \sim 1$, rather than the gradual decline observed experimentally.

The findings of Long and Anderson (1984) for linear polystyrene have been confirmed in subsequent studies in that laboratory, and shown to be relatively insensitive to solvent quality (Long and Anderson, 1985; Adamski and Anderson, 1987). The effects of branching have also been examined by comparing linear, comb-branched, and star-branched polystyrenes (Adamski and Anderson, 1987). For $\lambda > 1$ and at any given value of s, σ_f tended to be greater for the branched molecules. Flow-dependent rejection behavior has been reported also for a flexible polyanion (hydrolyzed polyacrylamide), in track-etched polycarbonate membranes (Munch et al., 1979).

Effects of concentration

Polymer chains begin to significantly interact at molar concentrations exceeding some threshold value C^*. One estimate of C^* is (Graessley, 1980):

$$C^* = \frac{1}{8N_A r_g^3} \tag{39}$$

where N_A is Avogadro's number. For $C_\infty > C^*$, the mean size of the polymer chains begins to decrease, suggesting a mechanism for increases in Φ and decreases in σ_f or σ_0 in addition to that discussed for rigid solutes. Long and Anderson (1985) found an inverse relationship between σ_f and C_∞ for large polystyrenes, for $C_\infty > C^*$ and constant s. The observed dependence of σ_f on C_∞ appeared to be less strong than predicted by scaling theory (Daoudi and Brochard, 1978). Guillot et al. (1985) examined the effects of concentration on the diffusion of polystyrene. For $\lambda > 1$ and $C_\infty > C^*$ they observed large increases in D/D_∞ with increasing C_∞, which they attributed primarily to the concentration dependence of Φ. A scaling analysis was presented to explain these results (Guillot et al., 1985).

The effects of polymer concentration on Φ, measured using controlled-pore glass, are qualitatively consistent with the findings for σ_f and D/D_∞ just discussed. It has been shown that Φ for polystyrene (Satterfield et al., 1978) and dextran (Brannon and Anderson, 1982) increases with C_∞. The complexity of the pore geometry in these partitioning studies, and the polydispersity of the dextran preparations used, makes quantitative interpretation of these results difficult. A scaling analysis of the effects of polymer concentration on partitioning was developed by Daoud and de Gennes (1977).

Conclusions

The hydrodynamic theory for the hindered transport of rigid, spherical molecules in capillary pores (cylinders, slits) is clearly at a mature stage. For very dilute solutions of neutral spheres, it is unlikely that additional analysis would lead to major new insights. In sharp contrast is the situation for nonspherical solutes and/or more concentrated solutions, where solute-pore and solute-solute hydrodynamic interactions remain largely unevaluated. Much additional work is needed also to understand and predict the rich and varied behavior of flexible polymers in fine pores.

Diffusion experiments using track-etched membranes have largely confirmed the predictions of the theory for dilute solutions of neutral spheres. Available results for diffusion of charged solutes also conform well with expectations. The limited data on convective transport of rigid solutes have shown less impressive quantitative agreement with the theory. A major difficulty in designing definitive experiments is in identifying macrosolutes or colloids that are indeed neutral, solid spheres. This difficulty emphasizes the need to obtain a better understanding of the effects of molecular configuration and of colloidal forces, so that more robust predictions can be made for various solute-pore combinations. One of the more important gaps in present knowledge concerns the prediction of the extent of polymer adsorption in pores and its effect on measurable transport properties.

Acknowledgment

Preparation of this review was supported in part by grants from the National Institutes of Health (DK 20368) and the Whitaker Health Sciences Fund.

Notation

C = molar concentration of solute in pore
$\langle C \rangle$ = molar concentration of solute averaged over pore cross section
C_∞ = solute concentration in bulk solution
$C_{i\infty}$ = solute concentration for ion i
C_0, C_L = solute concentrations in external solutions adjacent to membrane surfaces
C^* = critical concentration for overlap of polymer chains, Eq. 39
D = effective diffusivity for solute in pore, HD_∞
D_∞ = diffusivity in dilute bulk solution
E = interaction energy between solute and pore wall
F = Faraday's constant
f = volume fraction of solute in bulk solution
G = lag coefficient, Eq. 2
g = function describing axial concentration variations in pore, Eq. 7
H = hindrance factor for diffusion, Eq. 15
H^* = hindrance factor including Taylor dispersion, Eq. 26
h = half-width of slit pore
J_v = transmembrane volume flux, Eq. 20
K = enhanced drag coefficient, Eq. 2
K_c, K_d = integrals of inverse enhanced drag and lag coefficient, Eqs. 9, 10
K_s, K_t = hydrodynamic functions, Table 1
K_v = Taylor dispersion correction, Eqs. 26, 27
k = Boltzmann's constant
L = pore length
L_p = hydraulic permeability of membrane, Eq. 20
ℓ = Debye length, Eq. 29
M = molecular weight of solute
N = molar flux of solute in pore, axial direction
$\langle N \rangle$ = molecular flux averaged over pore cross section
N_A = Avogadro's number
ΔP = hydraulic pressure difference across membrane, "upstream" minus "downstream"
Pe = Peclet number based on pore length, Eq. 14
$\hat{Pe}$ = Peclet number based on pore radius, Eq. 28
Q = volume flow rate per pore
q_c = surface charge density on pore wall
q_s = surface charge density on spherical colloid
R = gas constant
r = radial position in pore (dimensional)
r_a, r_c, r_p = equivalent radii for noncircular pores, based on equal cross-sectional areas (r_a), largest inscribed circle (r_c), or equal partition coefficients (r_p)

r_g = radius of gyration of solute (polymer)
r_0 = radius of cylindrical pore
r_s = Stokes-Einstein solute radius, Eq. 1
s = dimensionless flow rate per pore, $\eta Q/kT$
T = temperature
U = solute velocity along pore axis
V = unperturbed solvent velocity
$\langle V \rangle$ = solvent velocity averaged over pore cross section
W = hindrance factor for convection (filtration), Eq. 16
Y_n = coefficients, Eq. 35
z = axial position in pore (dimensional)
z_i = valence of ion i

Greek letters

β = dimensionless radial position, r/r_0
γ = fraction of membrane surface occupied by pores
$\dot{\gamma}$ = characteristic rate of strain at pore entrance, $\langle V \rangle / r_0$
ϵ = dielectric permittivity of solvent
η = viscosity of solvent
$[\eta]$ = intrinsic viscosity of solute, zero-shear limit
λ = relative size of solute and pore, r_s/r_0 for cylinders, r_s/h for slits
$\Delta\Pi$ = osmotic pressure difference, $RT\ (C_0 - C_L)$ for dilute solutions
σ_f = reflection coefficient for filtration
σ_0 = reflection coefficient for osmosis
τ = time constant for slowest mode of relaxation of polymer coil, Eq. 38
Φ = partition coefficient, $\langle C \rangle / C_\infty$ at equilibrium

Appendix: Notes to the Text

1. In track-etch processes a thin sheet of material (usually mica or polycarbonate in 5–10 μm thicknesses) is first exposed to a source of heavy fission fragments. The energetic particles produce damage tracks in the material, allowing subsequent chemical etching to be highly directional. Pore number density and pore radius are controlled by the particle dose and etching conditions, respectively, and therefore can be varied independently. Pore radii as small as 30 Å have been achieved (Bean et al., 1970; Quinn et al., 1972). Pore cross sections are essentially circular in polycarbonate, rhombic in mica.

2. All of the results presented here assume that boundary layer resistances in the external solutions have been taken into account, so that the concentrations immediately adjacent to the membrane surfaces are known. Measurements of boundary layer resistances in stirred cells, including the effects of pore area fraction γ on mass transfer coefficients, have been reported by Malone and Anderson (1977) and Bohrer (1983).

3. The results of Weinbaum (1981) were reported in terms of "σ" ($= \sigma_f = 1 - W$) and a quantity "$\omega\bar{v}_s/L_p$". The latter quantity is equivalent to $(2/3)\lambda^2 H$.

4. The "theoretical" values for H ("D_m/D_0") reported by Van Bruggen et al. (1974) in their Table I, reportedly from the Renkin equation, appear to be in error. They are all significantly higher than those calculated using the present Eq. 24 and entry (1) of Table 1.

5. For comparisons of their theory with diffusion data, Adolf and Tirrell (1986) related I to r_s by equating values of Φ derived from their segment distributions with those obtained by Aubert and Tirrell (1982) for elastic dumbbells. However, Φ for the dumbbell model is greater than that for a random walk polymer, the difference at $r_g = r_0$ being some two orders of magnitude (Davidson et al., 1987). Furthermore, because Φ for the dumbbell model depends only on r_g, this approach seems to neglect the distinction between r_s and r_g.

Literature Cited

Adamski, R. P., and J. L. Anderson, "Solute Concentration Effect on Osmotic Reflection Coefficient," *Biophys. J.*, **44**, 79 (1983).

———, "Configurational Effects on Polystyrene Rejection from Microporous Membranes," *J. Polym. Sci.: Polym. Phys.*, **24** (1987).

Adolf, D. B., and M. Tirrell, "Concentration Effects on Averaged Transport Coefficients for Polymer Solutions in Narrow Pores," *J. Rheology*, **30**, 539 (1986).

Altenberger, A. R., and M. Tirrell, "On the Theory of Self-Diffusion in a Polymer Gel," *J. Chem. Phys.*, **80**, 2208 (1984).

Anderson, J. L., "Configurational Effect on the Reflection Coefficient for Rigid Solutes in Capillary Pores," *J. Theor. Biol.*, **90**, 405 (1981).

Anderson, J. L., and R. P. Adamski, "Solute Concentration Effects on Membrane Reflection Coefficients," *AIChE Symp. Ser.*, **79**(227), 84 (1983).

Anderson, J. L., and J. H. Brannon, "Concentration Dependence of the Distribution Coefficient for Macromolecules in Porous Media," *J. Polym. Sci.: Polym. Phys.*, **19**, 405 (1981).

Anderson, J. L., and D. M. Malone, "Mechanism of Osmotic Flow in Porous Membranes," *Biophys. J.*, **14**, 957 (1974).

Anderson, J. L., and J. A. Quinn, "Ionic Mobility in Microcapillaries. A Test for Anomalous Water Structures," *J. Chem. Soc. Faraday Trans. I*, **68**, 744 (1972).

———, "Restricted Transport in Small Pores. A Model for Steric Exclusion and Hindered Particle Motion," *Biophys. J.*, **14**, 130 (1974).

Aris, R., "On the Dispersion of a Solute in a Fluid Flowing through a Tube," *Proc. Roy. Soc. (Lond.)*, **A235**, 67 (1956).

Aubert, J. H., and M. Tirrell, "Effective Viscosity of Dilute Polymer Solutions Near Confining Boundaries," *J. Chem. Phys.*, **77**, 553 (1982).

Baltus, R. E., and J. L. Anderson, "Hindered Diffusion of Asphaltenes through Microporous Membranes," *Chem. Eng. Sci.*, **38**, 1959 (1983).

———, "Comparison of G. P. C. Elution Characteristics and Diffusion Coefficients of Asphaltenes," *Fuel*, **63**, 530 (1984).

Bean, C. P., "The Physics of Porous Membranes—Neutral Pores," *Membranes*, G. Eisenman, ed., Dekker, New York, **1**, 1 (1972).

Bean, C. P., M. V. Doyle, and G. Entine, "Etching of Submicron Pores in Irradiated Mica," *J. Appl. Phys.*, **41**, 1454 (1970).

Beck, R. E., and J. S. Schultz, "Hindrance of Solute Diffusion within Membranes as Measured with Microporous Membranes of Known Pore Geometry," *Biochim. Biophys. Acta*, **255**, 273 (1972).

Bohrer, M. P., "Diffusional Boundary Layer Resistance for Membrane Transport," *Ind. Eng. Chem. Fundam.*, **22**, 72 (1983).

Bohrer, M. P., W. M. Deen, C. R. Robertson, J. L. Troy, and B. M. Brenner, "Influence of Molecular Configuration on the Passage of Macromolecules across the Glomerular Capillary Wall," *J. Gen. Physiol.*, **74**, 583 (1979).

Bohrer, M. P., G. D. Patterson, and P. J. Carroll, "Hindered Diffusion of Dextran and Ficoll in Microporous Membranes," *Macromol.*, **17**, 1170 (1984).

Brannon, J. H., and J. L. Anderson, "Concentration Effects on Partitioning of Dextrans and Serum Albumin in Porous Glass," *J. Polym. Sci.: Polym. Phys.*, **20**, 857 (1982).

Brenner, H., and L. J. Gaydos, "The Constrained Brownian Movement of Spherical Particles in Cylindrical Pores of Comparable Radius," *J. Colloid Interf. Sci.*, **58**, 312 (1977).

Brinkman, H. C., "A Calculation of the Viscous Force Exerted by a Flowing Fluid on a Dense Swarm of Particles," *Appl. Sci. Res.*, **A1**, 27 (1947).

Brochard, F., and P. G. de Gennes, "Dynamics of Confined Polymer Chains," *J. Chem. Phys.*, **67**, 52 (1977).

Bungay, P. M., and H. Brenner, "The Motion of a Closely Fitting Sphere in a Fluid-Filled Tube," *Int. J. Multiph. Flow*, **1**, 25 (1973).

Cannell, D. S., and F. Rondelez, "Diffusion of Polystyrenes through Microporous Membranes," *Macromol.*, **13**, 1599 (1980).

Casassa, E. F., "Equilibrium Distribution of Flexible Polymer Chains between a Macroscopic Solution Phase and Small Voids," *J. Polym. Sci.: Polym. Lett.*, **5**, 773 (1967).

Casassa, E. F., and Y. Tagami, "An Equilibrium Theory for Exclusion Chromatography of Branched and Linear Polymer Chains," *Macromol.*, **2**, 14 (1969).

Cukier, R. I., "Diffusion of Brownian Spheres in Semidilute Polymer Solutions," *Macromol.*, **17,** 252 (1984).
Curry, F. E., "A Hydrodynamic Description of the Osmotic Reflection Coefficient with Application to the Pore Theory of Transcapillary Exchange," *Microvasc. Res.*, **8,** 236 (1974).
Curry, F. E., and C. C. Michel, "A Fiber Matrix Model of Capillary Permeability," *Microvasc. Res.*, **20,** 96 (1980).
Daoud, M., and P. G. de Gennes, "Statistics of Macromolecular Solutions Trapped in Small Pores," *J. Phys.* (Paris), **38,** 85 (1977).
Daoudi, S., and F. Brochard, "Flows of Flexible Polymer Solutions in Pores," *Macromol.*, **11,** 751 (1978).
Davidson, M. G., and W. M. Deen, "Hydrodynamic Theory for the Hindered Transport of Flexible Macromolecules in Porous Membranes," *J. Memb. Sci.* (1987).
Davidson, M. G., U. W. Suter, and W. M. Deen, "Equilibrium Partitioning of Flexible Macromolecules between Bulk Solution and Cylindrical Pores," *Macromol.*, **20,** 1141 (1987).
Deen, W. M., M. P. Bohrer, and B. M. Brenner, "Macromolecule Transport across Glomerular Capillaries: Application of Pore Theory," *Kidney Int.*, **16,** 353 (1979).
Deen, W. M., M. P. Bohrer, and N. B. Epstein, "Effects of Molecular Size and Configuration on Diffusion in Microporous Membranes," *AIChE J.*, **27,** 952 (1981).
Deen, W. M., C. R. Bridges, B. M. Brenner, and B. D. Myers, "Heteroporous Model of Glomerular Size-Selectivity: Application to Normal and Nephrotic Humans," *Am. J. Physiol.*, **249,** F374 (1985).
Deen, W. M., and F. G. Smith, III, "Hindered Diffusion of Synthetic Polyelectrolytes in Charged Microporous Membranes," *J. Memb. Sci.*, **12,** 217 (1982).
DiMarzio, E. A., and C. M. Guttman, "Separation by Flow," *Macromol.*, **3,** 131 (1970).
DuBois, R., and E. Stoupel, "Permeability of Artificial Membranes to a Pluridisperse Solution of ^{125}I-Polyvinylpyrrolidone," *Biophys. J.*, **16,** 1427 (1976).
Einstein, A., *Investigations on the Theory of the Brownian Movement,* R. Furth, ed., Dover, New York (1956).
Fanti, L. A., and E. D. Glandt, "Partition Equilibrium between a Bulk Phase and a Fibrous Membrane," Paper No. 85d, AIChE Ann. Meet., Miami (1986).
Ferry, J. D., "Statistical Evaluation of Sieve Constants in Ultrafiltration," *J. Gen. Physiol.*, **20,** 95 (1936).
———, *Viscoelastic Properties of Polymers,* 3rd ed. Wiley, New York, pp. 190, 195 (1980).
Fleischer, R. L., H. W. Alter, S. C. Furman, P. B. Price, and R. M. Walker, "Particle Track Etching," *Science,* **178,** 255 (1972).
Ganatos, P., R. Pfeffer, and S. Weinbaum, "A Strong Interaction Theory for the Creeping Motion of a Sphere between Plane Parallel Boundaries. 2: Parallel Motion," *J. Fluid Mech.*, **99,** 775 (1980).
Giddings, J. C., E. Kucera, C. P. Russell, and M. N. Myers, "Statistical Theory for the Equilibrium Distribution of Rigid Molecules in Inert Porous Networks. Exclusion Chromatography," *J. Phys. Chem.*, **72,** 4397 (1968).
Glandt, E. D., "Density Distribution of Hard Spherical Molecules inside Small Pores of Various Shapes," *J. Colloid Interf. Sci.*, **77,** 512 (1980).
———, "Distribution Equilibrium between a Bulk Phase and Small Pores," *AIChE J.*, **27,** 51 (1981a).
———, "Noncircular Pores in Model Membranes: A Calculation of the Effect of Pore Geometry on the Partition of a Solute," *J. Memb. Sci.*, **8,** 331 (1981b).
Graessley, W. W., "Polymer Chain Dimensions and the Dependence of Viscoelastic Properties on Concentration, Molecular Weight, and Solvent Power," *Polymer,* **21,** 258 (1980).
Guillot, G., L. Leger, and F. Rondelez, "Diffusion of Large Flexible Polymer Chains through Model Porous Membranes," *Macromol.* **18,** 2531 (1985).
Haberman, W. L., and R. M. Sayre, "Motion of Rigid and Fluid Spheres in Stationary and Moving Liquids Inside Cylindrical Tubes," David W. Taylor Model Basin Rept. No. 1143, U.S. Dept. Navy, Washington, DC (1958).
Happel, J., and H. Brenner, *Low Reynolds Number Hydrodynamics,* Nijhoff, The Hague (1983).
Hossain, M. M., D. D. Do, and J. E. Bailey, "Immobilization of Enzymes in Porous Solids under Restricted Diffusion Conditions," *AIChE J.*, **32,** 1088 (1986).
Idol, W. K., and J. L. Anderson, "Effects of Adsorbed Polyelectrolytes on Convective Flow and Diffusion in Porous Membranes," *J. Memb. Sci.*, **28,** 269 (1986).
Kathawalla, I. A., and J. L. Anderson, "Diffusion of Polymer Chains through Microporous Membranes," Paper No. 107g, AIChE Ann. Meet., Miami (1986).
Keh, H. J., and J. L. Anderson, "Boundary Effects on Electrophoretic Motion of Colloidal Spheres," *J. Fluid Mech.*, **153,** 417 (1985).
Klein, E., F. F. Holland, and K. Eberle, "Comparison of Experimental and Calculated Permeability and Rejection Coefficients for Hemodialysis Membranes," *J. Memb. Sci.*, **5,** 173 (1979).
Levitt, D. G., "General Continuum Analysis of Transport through Pores. I: Proof of Onsager's Reciprocity Postulate for Uniform Pore," *Biophys. J.*, **15,** 533 (1975a).
———, "General Continuum Analysis of Transport through Pores. II: Nonuniform Pores," *Biophys. J.*, **15,** 553 (1975b).
Lewellen, P. C., "Hydrodynamic Analysis of Microporous Mass Transport," Ph.D. Thesis, Univ. Wisconsin, Madison (1982).
Lightfoot, E. N., J. B. Bassingthwaighte, and E. F. Grabowski, "Hydrodynamic Models for Diffusion in Microporous Membranes," *Ann. Biomed. Eng.*, **4,** 78 (1976).
Long, T. D., and J. L. Anderson, "Flow-Dependent Rejection of Polystyrene from Microporous Membranes," *J. Polym. Sci.: Polym. Phys.*, **22,** 1261 (1984).
———, "Effects of Solvent Goodness and Polymer Concentration on Rejection of Polystyrene from Small Pores," *J. Polym. Sci.: Polym. Phys.*, **23,** 191 (1985).
Long, T. D., D. L. Jacobs, and J. L. Anderson, "Configurational Effects on Membrane Rejection," *J. Memb. Sci.*, **9,** 13 (1981).
Malone, D. M., and J. L. Anderson, "Diffusional Boundary-Layer Resistance for Membranes with Low Porosity," *AIChE J.*, **23,** 177 (1977).
———, "Hindered Diffusion of Particles through Small Pores," *Chem. Eng. Sci.*, **33,** 1429 (1978).
Mavrovouniotis, G. M., and H. Brenner, "Hindered Sedimentation and Dispersion Coefficients for Rigid, Closely Fitting Brownian Spheres in Circular Cylindrical Pores Containing Quiescent Fluids," Paper No. 85b, AIChE Ann. Meet., Miami (1986).
Mitchell, B. D., "Effects of Macromolecule Concentration and Charge on Membrane Rejection Coefficients," Ph.D. Thesis, Mass. Inst. Technol. (1984).
Mitchell, B. D., and W. M. Deen, "Theoretical Effects of Macromolecule Concentration and Charge on Membrane Rejection Coefficients," *J. Memb. Sci.*, **19,** 75 (1984).
———, "Effect of Concentration on the Rejection Coefficients of Rigid Macromolecules in Track-Etch Membranes," *J. Colloid Interf. Sci.*, **113,** 132 (1986).
Munch, W. D., L. P. Zestar, and J. L. Anderson, "Rejection of Polyelectrolytes from Microporous Membranes," *J. Memb. Sci.*, **5,** 77 (1979).
Ogston, A. G., "The Spaces in a Uniform Random Suspension of Fibers," *Trans. Faraday Soc.*, **54,** 1754 (1958).
Ogston, A. G., B. N. Preston, and J. D. Wells, "On the Transport of Compact Particles through Solutions of Chain Polymers," *Proc. Roy. Soc. (Lond.),* **A333,** 297 (1973).
Paine, P. L., and P. Scherr, "Drag Coefficients for the Movement of Rigid Spheres through Liquid-Filled Cylindrical Pores," *Biophys. J.*, **15,** 1087 (1975).
Pappenheimer, J. R., E. M. Renkin, and L. M. Borrero, "Filtration, Diffusion and Molecular Sieving through Peripheral Capillary Membranes," *Am. J. Physiol.*, **167,** 13 (1951).
Post, A. J., and E. D. Glandt, "Equilibrium Partitioning in Pores with Adsorbing Walls," *J. Colloid Interf. Sci.*, **108,** 31 (1985).
Prieve, D. C., and P. M. Hoysan, "Role of Colloidal Forces in Hydrodynamic Chromatography," *J. Colloid Interf. Sci.*, **64,** 201 (1978).
Quinn, J. A., J. L. Anderson, W. S. Ho, and W. J. Petzny, "Model Pores of Molecular Dimension. The Preparation and Characterization of Track-Etched Membranes," *Biophys. J.*, **12,** 990 (1972).
Reid, R. C., J. M. Prausnitz, and B. E. Poling, *Properties of Gases and Liquids,* 4th ed., McGraw-Hill, New York, 599 (1987).
Renkin, E. M., "Filtration, Diffusion, and Molecular Sieving through Porous Cellulose Membranes," *J. Gen. Physiol.*, **38,** 225 (1954).
Rodilosso, P. D., "Determination of the Partition Coefficient for Macromolecules in Porous Media: Potential Flows of Mass and Charge

about Solute Obstacles in Model Membranes," Ph.D. Thesis, Univ. Pennsylvania (1984).
Ruckenstein, E., and M. C. Tsai, "Optimum Pore Size for the Catalytic Conversion of Large Molecules," *AIChE J.*, **27**, 697 (1981).
Russel, W. B., "Brownian Motion of Small Particles Suspended in Liquids," *Ann. Rev. Fluid Mech.*, **13**, 425 (1981).
Satterfield, C. N., C. K. Colton, B. de Turckheim, and T. M. Copeland, "Effect of Concentration on Partitioning of Polystyrene within Finely Porous Glass," *AIChE J.*, **24**, 937 (1978).
Schultz, J. S., R. Valentine, and C. Y. Choi, "Reflection Coefficients of Homopore Membranes: Effect of Molecular Size and Configuration," *J. Gen. Physiol.*, **73**, 49 (1979).
Smith, D. M., "Restricted Diffusion through Pores with Periodic Constrictions," *AIChE J.*, **32**, 1039 (1986).
Smith, F. G., III, and W. M. Deen, "Electrostatic Double-Layer Interactions for Spherical Colloids in Cylindrical Pores," *J. Colloid Interf. Sci.*, **78**, 444 (1980).
———, "Electrostatic Effects on the Partitioning of Spherical Colloids between Dilute Bulk Solution and Cylindrical Pores," *J. Colloid Interf. Sci.*, **91**, 571 (1983).
Solomon, A. K., "Characterization of Biological Membranes by Equivalent Pores," *J. Gen. Physiol.*, **51**, 335s (1968).
Tanford, C., *Physical Chemistry of Macromolecules*, Wiley, New York (1961).
Taylor, G. I., "Dispersion of Soluble Matter in Solvent Flowing Slowly through a Tube," *Proc. Roy. Soc. (Lond.)*, **A219**, 186 (1953).
Van Bruggen, J. T., J. D. Boyett, A. L. van Bueren, and W. R. Galey, "Solute Flux Coupling in a Homopore Membrane," *J. Gen. Physiol.*, **63**, 639 (1974).
Wang, H., and R. Skalak, "Viscous Flow in a Cylindrical Tube Containing a Line of Spherical Particles," *J. Fluid Mech.*, **38**, 75 (1969).
Weinbaum, S., "Strong Interaction Theory for Particle Motion through Pores and Near Boundaries in Biological Flows at Low Reynolds Number," *Lect. Math. Life Sci.*, **14**, 119 (1981).
Wong H. J., and J. A. Quinn, "Hindered Diffusion of Macromolecules in Track-Etched Membranes," *Colloid and Interface Science*, **5**, M. Kerker, ed., Academic Press, New York, 169 (1976).
Wright, A. K., and M. R. Thompson, "Hydrodynamic Structure of Bovine Serum Albumin Determined by Transient Electric Birefringence," *Biophys. J.*, **15**, 137 (1975).
Yan, Z.-Y., S. Weinbaum, and R. Pfeffer, "On the Fine Structure of Osmosis Including Three-Dimensional Pore Entrance and Exit Behavior," *J. Fluid Mech.*, **162**, 415 (1986).
Yavorsky, D. P., "Static and Hydrodynamic Studies of the Conformation of an Adsorbed Macromolecule at the Solid/Liquid Interface," Ph.D. Thesis, Univ. Pennsylvania (1981).
Zeman, L., and M. Wales, "Steric Rejection of Polymeric Solutes by Membranes with Uniform Pore Size Distribution," *Separ. Sci. Technol.*, **16**, 275 (1981).

Manuscript received Mar. 17, 1987, and revision received June 4, 1987.

William M. Deen *is a native of Seattle and did his undergraduate work in chemical engineering at Columbia University, graduating in 1969. He received a Ph.D. from Stanford University in 1973, following completion of thesis research with Channing Robertson on the modeling of mass transfer in the kidney microcirculation. Intrigued by the possibilities of using chemical engineering principles to better understand renal physiology and kidney disease, he then spent two years as a postdoctoral fellow in the nephrology laboratory of Barry M. Brenner, and one year as a faculty member in physiology, both at the University of California, San Francisco. He joined the faculty at M.I.T. in 1976. His research interests continue to center on transport phenomena in biological systems. His teaching focus has been on undergraduate and graduate courses in fluid mechanics and heat and mass transfer. Among his nonprofessional interests are folk music (acoustic guitar), hiking, and cross-country skiing. He has an avid interest in railroad history and preservation, and will go to great lengths to see and photograph operating steam locomotives. This avocation is gracefully tolerated by his wife, and increasingly abetted by his young son.*